

# MIXED PRECISION ITERATIVE REFINEMENT WITH SPARSE APPROXIMATE INVERSE PRECONDITIONING

ERIN CARSON\* AND NOAMAN KHAN†

**Abstract.** With the commercial availability of mixed precision hardware, mixed precision GMRES-based iterative refinement schemes have emerged as popular approaches for solving sparse linear systems. Existing analyses of these approaches, however, are all based on using a full LU factorization to construct preconditioners for use within GMRES in each refinement step. In practical applications, inexact preconditioning techniques, such as incomplete LU or sparse approximate inverses, are often used for performance reasons.

In this work, we investigate the use of sparse approximate inverse preconditioners within GMRES-based iterative refinement. We analyze the computation of sparse approximate inverses in finite precision and derive constraints under which the user-specified stopping criteria will be satisfied. We then analyze the behavior of and convergence constraints for a GMRES-based iterative refinement scheme that uses sparse approximate inverse preconditioning, which we call SPAI-GMRES-IR. Our numerical experiments confirm that in some cases, sparse approximate inverse preconditioning can have an advantage over using a full LU factorization.

**Key words.** mixed precision, GMRES, iterative refinement, approximate preconditioners, sparse linear systems

**AMS subject classifications.** 65F08, 65F10, 65F50, 65G50, 65Y99

**1. Introduction.** We consider the problem of solving linear systems  $Ax = b$  with a nonsingular  $n \times n$  matrix  $A$ . With the recent emergence of commercially available mixed precision hardware, there has been a renewed interest in the development of mixed precision algorithms for numerical linear algebra. The benefit of using low precision is that it is much faster and more energy efficient. Compared to double precision, for example, using half precision tensor cores available on modern NVIDIA GPUs leads to a theoretical  $16\times$  improvement in performance. Low precision can also reduce communication and memory bottlenecks, since we need to move and store fewer bits. The downside is that with fewer bits, we have less accuracy and a smaller range of representable numbers. The size in bits, range, and unit roundoff  $u$  are given for four IEEE precisions in Table 1.1.

Table 1.1: Parameters for IEEE floating point precisions. The range denotes the order of magnitude of the largest and smallest positive normalized floating point numbers.

Type	Size	Range	Unit Roundoff $u$
half	16 bits	$10^{\pm 5}$	$2^{-11} \approx 4.9 \cdot 10^{-4}$
single	32 bits	$10^{\pm 38}$	$2^{-24} \approx 6.0 \cdot 10^{-8}$
double	64 bits	$10^{\pm 308}$	$2^{-53} \approx 1.1 \cdot 10^{-16}$
quad	128 bits	$10^{\pm 4932}$	$2^{-113} \approx 9.6 \cdot 10^{-35}$

The goal is thus to design mixed precision approaches which use lower precision in select computations and higher precision in others, in such a way that both (1)

---

\* Faculty of Mathematics and Physics, Charles University. Both authors were supported by Charles University PRIMUS project no. PRIMUS/19/SCI/11. The first author was additionally supported by Charles University Research program no. UNCE/SCI/023 and by the Exascale Computing Project (17-SC-20-SC), a collaborative effort of the U.S. Department of Energy Office of Science and the National Nuclear Security Administration.

performance is improved and (2) the attainable accuracy remains sufficient; see [1] for a recent survey of these efforts. For the problem of solving linear systems, mixed precision iterative refinement has been the focus of renewed attention. The general idea behind iterative refinement is to compute an initial solution  $x_0$  to  $Ax = b$ , and then to perform some  $i$  iterations, computing the residual  $r_i = b - Ax_i$ , solving  $Ad_i = r_i$ , and then updating the approximate solution  $x_{i+1} = x_i + d_i$ . Typically, an LU factorization of  $A$  is computed at the beginning, which is used to solve for  $x_0$ , and then reused in each iteration to solve for the correction  $d_i$ . We call this LU-based variant “standard IR”.

There is a long history of using mixed precision within iterative refinement. What we call “traditional” iterative refinement involves computing the residuals in double the working precision  $u$ , which was used already by Wilkinson in 1948 [36], and was analyzed by Wilkinson [37] and Moler [32]. Fixed precision iterative refinement, in which all computations are performed in precision  $u$ , was analyzed by Jankowski and Woźniakowski [28] and Skeel [35]. Motivated by the faster speed of single precision versus double, in the early 2000s, there was a flurry of work in using lower precision in the computation of the LU factorization, which is the most expensive part of the computation, and the working precision elsewhere; see, for example, [29], [2, Section 9]. See [11, Table 1.1] for a summary.

The inclusion of half precision in modern GPUs inspired the development of iterative refinement schemes that use three or more hardware precisions. In [11], the authors define an iterative refinement scheme which uses three potentially different precisions:  $u_f$  for the factorization,  $u$  for the working precision, and  $u_r$  for the residual computation. To allow for general solvers for the correction term  $d_i$ , the authors also introduce a fourth precision  $u_s$ , which denote the “effective precision” of the solve. For standard iterative refinement, the effective precision of the solve (which involves triangular solves with the LU factors computed in precision  $u_f$ ), we have  $u_s = u_f$ . Then assuming that  $u_f \geq u$  and  $u_r \leq u^2$ , the relative forward and backward errors in standard iterative refinement will converge to level  $u$  when  $\kappa_\infty(A) \leq u_f^{-1}$ .

The reason for introducing this effective precision becomes clear when we use a more accurate solver. The GMRES-based iterative refinement scheme (GMRES-IR) introduced in [10] uses GMRES left preconditioned by the computed LU factors in order to solve for  $d_i$  in each refinement step. Assuming that GMRES is executed in working precision  $u$ , with the matrix-vector products with the preconditioned matrix computed in precision  $u^2$ , GMRES-IR is guaranteed to give forward and backward errors to the working precision for more ill-conditioned systems than standard iterative refinement. Again under the assumption that  $u_f \geq u$  and  $u_r \leq u^2$ , the relative forward and backward errors in GMRES-IR will converge to level  $u$  when  $\kappa_\infty(A) \leq u^{-1/2}u_f^{-1}$ .

This requirement that the preconditioned matrix is applied in double the working precision within GMRES is unattractive from a performance perspective. In [3], the authors introduce and analyze a five-precision variant of GMRES-IR. In addition to the working precision  $u$ , factorization precision  $u_f$ , and residual precision  $u_r$  for the refinement scheme, they also add precisions  $u_g$  for the working precision within GMRES and  $u_p$  for the precision in which the precondition matrix is applied to a vector within GMRES. Setting  $u = u_g = u_p$  is a variant commonly used in practice. The cost is that this variant is only guaranteed to converge. For this particular variant, again assuming that  $u_f \geq u$  and  $u_r \leq u^2$ , we obtain relative forward and backward errors to the level of the working precision for matrices with  $\kappa_\infty(A) \leq u^{-1/3}u_f^{-2/3}$ .

The original analysis of GMRES-IR makes the assumption that a full LU fac-

torization is computed for use as a left preconditioner in GMRES in each refinement step. This is often undesirable from a performance perspective in the case of sparse  $A$ . Even if  $A$  is very sparse, its LU factors may have considerable fill-in. In practice, one would like to use a preconditioner that is considerably sparse, but still effective enough at improving convergence behavior.

In this work, we explore the potential for the use of sparse approximate inverse preconditioners within mixed precision GMRES-IR. In Section 2 we give a brief background on sparse approximate inverse preconditioning and discuss approaches related to the present work. In Section 3, we analyze errors in constructing the sparse approximate inverse in finite precision and then analyze the behavior of both standard and GMRES-based iterative refinement schemes based on sparse approximate inverses, giving theoretical results on attainable accuracy and criteria for convergence of the refinement scheme. In Section 4 we present numerical experiments and in Section 5 we discuss open problems and future work.

## 2. Background and related work.

**2.1. Notation.** We first introduce notation which will be used in the remainder of the text. Of particular importance will be various condition numbers. For a given norm  $p$ , a matrix  $A$  and a vector  $x$  we define

$$\kappa_p(A) = \|A^{-1}\|_p \|A\|_p, \quad \text{cond}_p(A) = \| |A^{-1}| |A| \|_p, \quad \text{cond}_p(A, x) = \frac{\| |A^{-1}| |A| x \|_p}{\|x\|_p},$$

where  $|A| = (|a_{ij}|)$ . In the case that  $p$  is not specified, the infinity norm should be assumed. We will use  $u$ 's to denote unit roundoffs, where subscripts on  $u$  will distinguish between various precisions. For rounding error analysis, we will frequently use the notation

$$\gamma_k = \frac{ku}{1 - ku}, \quad \tilde{\gamma}_k = \frac{cku}{1 - cku},$$

where  $c$  is a small constant independent of problem dimension and  $u$  is the unit roundoff. A superscript on  $\gamma$  indicates that  $u$  has that superscript as a subscript, e.g.,  $\gamma_k^f = ku_f/(1 - ku_f)$ . Quantities computed in finite precision will be denoted with hats. In order to make clear the distinction between iterative refinement (the outer solver) and GMRES (the inner solver), we will always use the word ‘‘steps’’ when referring to iterative refinement and ‘‘iterations’’ when referring to GMRES.

**2.2. Sparse approximate inverse preconditioners.** The idea behind sparse approximate inverse (SPAI) preconditioning is to explicitly construct a matrix  $M \approx A^{-1}$ . This has advantages within Krylov subspace methods since the application of the preconditioner only involves a matrix-vector product, rather than, e.g., the triangular solves involved when using LU-based preconditioners. There are many possible algorithms for computing  $M$ ; see [9, 7] for a survey of references.

For computing a sparse approximate inverse in unfactored form (i.e., a single matrix  $M$ ), a popular approach is based on Frobenius norm minimization, in which  $M$  is computed as a solution to  $\min_{M \in \mathcal{S}} \|I - AM\|_F$ , for a set of sparse matrices  $\mathcal{S}$ . Computation of  $M$  thus reduces to solving a linear least squares problem for each column  $m_k$  of  $M$ . A primary advantage for performance is that these linear least squares problems are independent, and thus can be solved in parallel.

The set  $\mathcal{S}$  can be prescribed by fixing a sparsity pattern for  $M$ , and this is indeed the technique that was used in early work. It is difficult, however, in general,

to select a priori a sparsity pattern which will produce an effective preconditioner. Motivated by this, authors have developed iterative approaches, in which one starts with an initial sparsity structure and adds nonzeros to this pattern until the constraint  $\|e_k - Am_k\|_2 \leq \varepsilon$  is satisfied for some threshold  $\varepsilon$  or a maximum number of nonzeros has been reached. For algorithms of this type, see, e.g., the work of Cosgrove et al. [13], Grote and Huckle [20], and Gould and Scott [18].

The algorithm of Grote and Huckle, shown in Algorithm 2.1, is among the most commonly used, and is the focus of our present work here. Motivated by the difficulty of selecting a sparsity pattern that results in a good preconditioner a priori, the idea of [20] was to develop an adaptive technique which captures the most important nonzero indices dynamically. The algorithm takes as input the matrix  $A$ , an initial sparsity pattern  $J$ , parameter  $\varepsilon$  as a convergence tolerance,  $\alpha$ , which gives the maximum number of iterations for each column, and  $\beta$ , which gives the maximum number of nonzeros that are added to the pattern in each iteration.

Despite that each column can be computed in parallel, constructing an SPAI preconditioner is often costly, especially for large-scale problems; see, e.g., [6, 9, 12, 16]. The memory requirements for SPAI scale quadratically and the computational cost cubically in the number of nonzeros per row [16]. The development of efficient sparse approximate inverse computations for modern hardware, especially GPUs, has been the subject of much recent work; see, e.g., [17, 31, 15, 21].

We note that there are also techniques based on incomplete biconjugation which can be used to produce sparse triangular factors, so that the approximate inverse is a product of two matrices approximating the LU factors of  $A$ ; see, e.g., [8]. Here we do not consider this approach nor the many other variants of sparse approximate inverses, including factorized sparse approximate inverses [26], modified sparse approximate inverses [27], or incomplete sparse approximate inverses [5]. We note that these could be interesting venues for extending the present work.

**2.3. Mixed precision iterative refinement.** In Algorithm 2.2 we present a general three-precision iterative refinement scheme as presented in [11]. There are three hardware precisions involved:  $u_f$ , in which the LU factorization of  $A$  is computed,  $u_r$ , in which the residual is computed, and  $u$ , the working precision in which all other computations are performed. The effective precision  $u_s$  for the solver in line 5 of Algorithm 2.2 depends on the precisions and the solver used. In particular,  $u_s$  is defined such that the solver satisfied three conditions:

$$(2.1) \quad \hat{d}_i = (1 + u_s E_i) d_i, \quad u_s \|E_i\|_\infty < 1,$$

$$(2.2) \quad \|\hat{r}_i - A\hat{d}_i\|_\infty \leq u_s (c_1 \|A\|_\infty \|\hat{d}_i\|_\infty + c_2 \|\hat{r}_i\|_\infty),$$

$$(2.3) \quad |\hat{r}_i - A\hat{d}_i| \leq u_s G_i |\hat{d}_i|,$$

where  $E_i$ ,  $c_1$ ,  $c_2$ , and  $G_i$  are functions of  $n$ ,  $A$ ,  $\hat{r}_i$ , and  $u_s$  and have nonnegative entries, and here and in the remainder of the text hats denote quantities computed in finite precision. These three conditions are used in analyzing the relative forward, normwise backward, and componentwise backward errors, respectively. The authors in [11] derive these quantities for two different solvers: 1) triangular solves using the computed LU factors (SIR), and 2) left-preconditioned GMRES, where the computed LU factors are used as preconditioners and the preconditioners and preconditioned coefficient matrix are applied to vectors in double the working precision (GMRES-IR). We summarize the results of the analysis in Table 2.1; see [11, Table 2.1].

Given a choice of solver with a particular  $u_s$  along with precisions  $u_f$ ,  $u$ , and

---

**Algorithm 2.1** Sparse approximate inverse (SPAI)

---

**Input:**  $A \in \mathbb{R}^{n \times n}$ ,  $J \in \mathbb{B}^{n \times n}$ ,  $\alpha \geq 0$ ,  $\beta \geq 0$ ,  $\varepsilon > 0$

**Output:** Right preconditioner  $M \approx A^{-1}$ ,  $M \in \mathbb{R}^{n \times n}$

```
1: for  $k \leftarrow 1$  to  $n$  do
2:    $e_k \leftarrow I(:, k)$ 
3:    $J_k \leftarrow J(:, k)$ 
4:   for step  $\leftarrow 0$  to  $\alpha$  do
5:      $I_k \leftarrow \left\{ i \in \{1, \dots, n\} : \sum_{j \in J_k} |a_{ij}| \neq 0 \right\}$ 
6:      $\bar{A}_k \leftarrow A(I_k, J_k)$ 
7:      $\bar{e}_k \leftarrow e_k(I_k)$ 
8:      $\bar{Q}, \bar{R} \leftarrow qr(\bar{A}_k)$ 
9:      $\bar{M}_k \leftarrow \bar{R}^{-1} \bar{Q}^T \bar{e}_k$ 
10:     $\bar{r}_k \leftarrow \bar{A}_k \bar{M}_k - \bar{e}_k$ 
11:    if  $\|\bar{r}_k\|_2 < \varepsilon$  then
12:      break
13:    end if
14:     $L_k \leftarrow I_k \cup \{k\}$ 
15:    for  $\ell \in L_k$  do
16:       $N_\ell \leftarrow \{j : a_{\ell j} \neq 0\}$ 
17:    end for
18:     $\tilde{J}_k \leftarrow \bigcup_{\ell \in L_k} N_\ell$ 
19:     $\tilde{\rho}_k \leftarrow 0$ 
20:    for  $j \in \tilde{J}_k$  do
21:       $\rho_{jk} \leftarrow (\|\bar{r}_k\|_2^2 - \frac{[\bar{r}_k^T A_j(I_k)]^2}{\|A_j(I_k)\|_2^2})^{\frac{1}{2}}$ 
22:       $\tilde{\rho}_k \leftarrow \tilde{\rho}_k + \rho_{jk}$ 
23:    end for
24:     $\tilde{\rho}_k \leftarrow \frac{\tilde{\rho}_k}{|J_k|}$ 
25:    for idx  $\leftarrow 1$  to  $\beta$  do
26:       $j \leftarrow \operatorname{argmin}_{j \in \tilde{J}_k} \rho_{jk}$ 
27:       $J_k \leftarrow J_k \cup \{j : \rho_{jk} \leq \tilde{\rho}_k\}$ 
28:       $\tilde{J}_k \leftarrow \tilde{J}_k \setminus \{j\}$ 
29:    end for
30:  end for
31:   $M_k(J_k) \leftarrow \bar{M}_k$ 
32: end for
```

---

$u_r$ , the authors in [11] prove the following results about the behavior of the resulting iterative refinement scheme.

**THEOREM 2.1.** [11, Corollary 3.3] *Let Algorithm 2.2 be applied to a linear system  $Ax = b$  where  $A$  is  $n \times n$  and nonsingular with at most  $p$  nonzeros per row and assume the solver used satisfies (2.1). Then for refinement step  $i \geq 0$ , as long as*

$$(2.4) \quad \phi_i = 2u_s \min(\operatorname{cond}(A), \kappa_\infty(A)\mu_i) + u_s \|E_i\|_\infty$$

*is less than 1, the forward error is reduced on the  $i$ th step by a factor of approximately*

---

**Algorithm 2.2** General Iterative Refinement Scheme

---

**Input:**  $n$ -by- $n$  nonsingular matrix  $A$  and length- $n$  right-hand side vector  $b$ .

**Output:** Approximate solution  $\hat{x}$  to  $Ax = b$ .

- 1: Compute LU factorization of  $A$  in precision  $u_f$ .
  - 2: Solve  $Ax_0 = b$  in precision  $u_f$ ; store  $x_0$  in precision  $u$ .
  - 3: **for**  $i = 0, 1 \dots$  until convergence **do**
  - 4:   Compute  $r_i = b - Ax_i$  in precision  $u_r$ ; store  $r_i$  in precision  $u$ .
  - 5:   Solve  $Ad_i = r_i$  at effective precision  $u_s$ ; store  $d_i$  in precision  $u$ .
  - 6:   Update  $x_{i+1} = x_i + d_i$  in precision  $u$ .
  - 7: **end for**
- 

Table 2.1: Summary of sizes of quantities in the assumptions (2.1)-(2.3) as given in [11, Table 2.1]. In the table,  $f(n) = O(n^2)$ .

	$u_s \ E_i\ _\infty$	$u_s \max(c_1, c_2)$	$u_s \ G_i\ _\infty$
SIR	$3nu_f \ A^{-1}\  \ \hat{L}\  \ \hat{U}\ _\infty$	$3nu_f \frac{\ \hat{L}\  \ \hat{U}\ _\infty}{\ A\ _\infty}$	$3nu_f \ \hat{L}\  \ \hat{U}\ _\infty$
GMRES-IR	$uf(n)(1 + nu_f \kappa(A))^2$	$O(u)$	$O(u) \ A\ _\infty$

$\phi$  until an iterate  $\hat{x}$  is obtained for which

$$\frac{\|x - \hat{x}\|_\infty}{\|x\|_\infty} \lesssim 4pu_r \text{cond}(A, x) + u.$$

The quantity  $\mu_i$  in the above Theorem is defined such that

$$\|A(x - \hat{x}_i)\|_\infty = \mu_i \|A\|_\infty \|x - \hat{x}_i\|_\infty,$$

where  $\mu_i$  satisfies  $\kappa_\infty(A)^{-1} \leq \mu_i \leq 1$ . The insight in [10] is that  $\mu_i$  will be very small at the beginning of the refinement process, and will only grow close to its maximum once the process is close to convergence.

**THEOREM 2.2.** [11, Corollary 4.2] *Let Algorithm 2.2 be applied to a linear system  $Ax = b$  where  $A$  is  $n \times n$  and nonsingular with at most  $p$  nonzeros per row and assume the solver used satisfies (2.1). Then for refinement step  $i \geq 0$ , as long as*

$$(2.5) \quad \phi_i = (c_1 \kappa_\infty(A) + c_2) u_s$$

*is less than 1, the residual is reduced in each step by a factor of approximately  $\phi$  until an iterate  $\hat{x}$  is obtained for which*

$$\|b - A\hat{x}\|_\infty \lesssim pu(\|b\|_\infty + \|A\|_\infty \|\hat{x}\|_\infty),$$

*which indicates that  $\hat{x}$  is a backward stable solution to the working precision.*

For simplicity, we will only consider normwise forward and backward errors in this work, but direct the reader to [11, Section 5] for detailed treatment of componentwise backward error.

In the case of standard iterative refinement, these theorems say that the forward and backward errors will converge as long as  $\kappa_\infty(A) \leq u_f^{-1}$ , with a limiting value of  $pu_r + u$  for the backward error and a limiting value of  $pu_r \text{cond}(A, x) + u$  for the forward error. GMRES-IR will have the same limiting values, but looser constraints

on condition number; for the backward error, we require  $\kappa_\infty(A) \leq u^{-1/2}u_f^{-1/2}$  (see [3, Table 2.1]) and for the forward error, we require  $\kappa_\infty(A) \ll u^{-1/2}u_f^{-1}$ . Note that in the case that  $u_r = u^2$ , the constraint for backward error convergence in GMRES also becomes  $\kappa_\infty(A) \leq u^{-1/2}u_f^{-1}$  since the backward error is bounded by the forward error.

In the recent work [3], it was shown that for the variant of GMRES-IR where GMRES is computed in entirely the working precision (i.e., no extra precision is used in applying the preconditioned matrix), the constraint for convergence of the forward error to the limiting value is  $\kappa_\infty(A) \leq u^{-1/3}u_f^{-2/3}$  and that for the backward error is  $\kappa_\infty(A) \leq u^{-1/3}u_f^{-1/3}$ .

**2.4. Related Work.** Along with the resurgence of interest in mixed precision iterative refinement have come a number of works that build on and expand the work on GMRES-based iterative refinement in, e.g., [10, 11, 2, 3]. In [23], Higham and Mary develop a new general preconditioning technique based on a low-rank approximation of the error  $E = \hat{U}^{-1}\hat{L}^{-1}A - I$ , where  $\hat{L}$  and  $\hat{U}$  are approximate LU factors of  $A$ . A randomized SVD is used to produce this low-rank approximation, and the preconditioner is applied in the context of GMRES-IR. This technique can apply to the case where the approximation in LU is due to low precision computation, as well as other sources of error including using an incomplete LU factorization and a block low-rank LU factorization. See [4, 24] for other theoretical and experimental results on the use of block low-rank LU factorization preconditioners within iterative refinement.

In [30], Lindquist, Luszczek, and Dongarra have recently evaluated mixed precision restarted GMRES (equivalent in some sense to a variant of GMRES-IR) on a GPU-accelerated node with various preconditioners. They found that the use of incomplete LU with zero fill-in (ILU(0)) resulted in unfavorable performance (a slowdown on average). The authors attribute this partially to the fact that sparse triangular solves have limited parallelism for the GPU to exploit.

In the recent work [4], Amestoy et al. extend the work on GMRES-based iterative refinement to LU factorization methods more appropriate for sparse matrices, including those based on block low-rank approximations and on static pivoting strategies.

The present work differs from these recent approaches in that we depart from the restriction to preconditioning based on LU factorization and instead look at sparse approximate inverses as preconditioners within mixed precision GMRES-based iterative refinement. In the following section, we will first analyze the numerical properties of SPAI preconditioners computed in a given precision with given parameters, and then evaluate the constraints for convergence of GMRES-IR with SPAI preconditioners.

**3. Analysis of SPAI-based iterative refinement.** Our ultimate goal is to prove conditions under which the SPAI-GMRES-IR algorithm (Algorithm 3.1) will converge and to determine how the precision  $u_f$  and approximation parameter  $\varepsilon$  should be related. We first give bounds on the quality of the SPAI preconditioner when it is computed in finite precision, analogous to those given for the case of exact arithmetic in [20].

Suppose we want to construct a sparse approximate inverse of a nonsingular matrix  $A$  for use as a left preconditioner, which we will denote  $M$ . That is, instead of solving  $Ax = b$  we will solve  $MAx = Mb$ . We will do so using the algorithm of Grote and Huckle [20] (see Algorithm 2.1), executed in some precision  $u_f$ . This algorithm as stated produces a right preconditioner for  $A$ . We can obtain a left preconditioner by executing the algorithm on  $A^T$  and then transposing the obtained approximate



inverse, i.e.,  $M \leftarrow M^T$ . We will denote the version of  $M$  computed in finite precision as  $\widehat{M}$ .

In contrast to how the method is often used in practice, we will not specify a maximum number of nonzeros here (i.e., in the extreme case we could allow a fully dense inverse). More important for our purposes will be the assumption that for each column  $\widehat{m}_k^T$  of  $\widehat{M}^T$ , it holds that

$$(3.1) \quad \|e_k - A^T \widehat{m}_k^T\|_2 \leq \varepsilon.$$

The way the SPAI algorithm works, we keep iterating, computing a QR factorization of some submatrix  $\bar{A}^T$  of  $A^T$  (selected by specifying a particular set of row and column indices) and solving the least squares problem  $\min_{\bar{m}_k^T} \|\bar{A}^T \bar{m}_k^T - \bar{e}_k\|_2$ . The vector  $\bar{m}_k^T$  then gives the nonzero entries in column  $k$  of  $M^T$  (corresponding to the same indices as the rows of  $A^T$  selected to construct  $\bar{A}^T$ ). Row and column indices are added to the set, and the iteration is continued until  $\min_{\bar{m}_k^T} \|\bar{A}^T \bar{m}_k^T - \bar{e}_k\|_2 \leq \varepsilon$ , which indicates that (3.1) holds.

We assume that all computations within the SPAI algorithm are performed in a precision  $u_f$ . We make the simplifying assumption that the QR factorization of  $\bar{A}^T$  is computed fully, but note that in practice one only needs to compute a QR factorization of a smaller block corresponding to the newly added indices; see, e.g., [34, Algorithm 5]. We further assume that the QR factorization is computed using Householder QR (or a method with similar numerical properties, like TSQR).

There are two interesting questions we can ask:

1. Assuming we impose no maximum sparsity pattern on  $\widehat{M}$ , i.e., we keep adding rows and columns of  $A^T$  until  $\|r_k\|_2 = \|\bar{e}_k - \bar{A}^T \bar{m}_k^T\|_2 \rightarrow 0$  for the computation in exact arithmetic, under what constraint on  $u_f$  can we say that  $\|\widehat{r}_k\|_2 \leq \varepsilon$ , with  $\widehat{r} = fl_{u_f}(e_k - A^T \widehat{m}_k^T)$  for the computed  $\widehat{m}_k^T$ ?
2. Assume that when  $M$  is computed in exact arithmetic, we quit when  $\|r_k\|_2 \approx \varepsilon$ . For  $\widehat{M}$  computed in precision  $u_f$  with the same sparsity pattern as  $M$ , what is  $\|e_k - A^T \widehat{m}_k^T\|_2$ ?

The first question is more relevant for our use case, since in practice we must use some stopping criteria to stop the algorithm. While the second question is interesting, we usually will not know in practice the minimal sparsity pattern for the exactly computed  $M$  that satisfies our  $\varepsilon$  constraint.

We first tackle the first question. Here we will assume that no overflow or underflow occurs during the SPAI computation in precision  $u_f$ . We note that to mitigate the risk of this one could use sophisticated scaling techniques such as those described in [25]; we leave the development of particular scaling techniques for low precision SPAI construction as future work. To account for finite precision error, it suffices to assume that we are on the final iteration for column  $k$ , after which we will quit since the condition  $\|\widehat{r}_k\|_2$  is satisfied. Using the backward error result [22, Theorem 20.3], which says that the computed solution  $\widehat{m}_k^T$  is the exact least squares solution to

$$\min_{\bar{m}_k^T} \|(e_k + \Delta e_k) - (A^T + \Delta A^T) \bar{m}_k^T\|_2,$$

where  $|\Delta A^T| \leq n \tilde{\gamma}_n^f e e^T |A^T|$  and  $|\Delta e_k| \leq n \tilde{\gamma}_n^f e e^T |e_k|$ , we can then bound

$$(3.2) \quad \|e_k - A^T \widehat{m}_k^T\|_2 \leq n^2 \tilde{\gamma}_n^f (\|e_k\| + |A^T| \|\widehat{m}_k^T\|_2 + (1 + n^2 \tilde{\gamma}_n^f \text{cond}_2(A)) \|r_k\|_2 + O(u_f^2)),$$



where  $r_k = e_k - A^T m_k^T$ . Then using standard rounding error analysis, we have

$$\|\hat{r}_k\|_2 \leq \|e_k - A^T \hat{m}_k^T\|_2 + \|\Delta \hat{r}_k\|_2,$$

where  $\|\Delta \hat{r}_k\|_2 \leq \tilde{\gamma}_n^f \|e_k\| + |A^T| \|\hat{m}_k^T\|_2$ . Then

$$\|\hat{r}_k\|_2 \leq n^2 \tilde{\gamma}_n^f \|e_k\| + |A^T| \|\hat{m}_k^T\|_2 + (1 + n^2 \tilde{\gamma}_n^f \text{cond}_2(A)) \|r_k\|_2 + O(u_f^2),$$

where the  $\|\Delta \hat{r}_k\|_2$  factor has been absorbed into the  $\tilde{\gamma}_n^f$  in the first term on the right-hand side.

Now, in theory, we could keep increasing the size of the subproblem in solving for the column of the inverse until we have the full matrix  $A^T$ , which would mean that  $r_k = 0$ . Thus we can consider this term to be vanishing, and we are left with (ignoring higher order terms)

$$\|\hat{r}_k\|_2 \leq n^2 \tilde{\gamma}_n^f \|e_k\| + |A^T| \|\hat{m}_k^T\|_2.$$

Then in order to guarantee that we will eventually iterate to a solution with  $\|\hat{r}_k\|_2 \leq \varepsilon$ , we should have

$$(3.3) \quad n^2 \tilde{\gamma}_n^f \|e_k\| + |A^T| \|\hat{m}_k^T\|_2 \leq \varepsilon.$$

In other words, the problem must not be so ill-conditioned such that we can not guarantee that we incur an error less than  $\varepsilon$  just computing the residual. We note that we could turn this into the more descriptive bound

$$\text{cond}_2(A^T, m_k^T) \lesssim \varepsilon u_f^{-1},$$

as well as an a priori bound of the form

$$(3.4) \quad \text{cond}_2(A^T) \lesssim \varepsilon u_f^{-1}.$$

We note that this is likely quite pessimistic in practice. Note that  $\text{cond}_2(A^T)$  can be considerably smaller than  $\kappa_2(A)$ . We also note that the  $n$  factors here and in the following bounds can be a large overestimate, since we in practice solve the least squares problem with the smaller submatrix  $\bar{A}^T$ . Perhaps a more useful way to think about (3.4) is that with a given matrix  $A$  and a chosen precision  $u_f$ , in order to guarantee success of the SPAI algorithm, one must set  $\varepsilon$  such that  $\varepsilon \geq u_f \text{cond}_2(A^T)$ .

This analysis echoes what we may intuitively think: the larger we make  $\varepsilon$  (meaning the more approximate the inverse), the larger the  $u_f$  we can tolerate. If we require smaller  $\varepsilon$ , meaning we want a better quality preconditioner, then we must have a smaller  $u_f$  to match.

Given that (3.3) is satisfied, we know that we can find a computed solution  $\hat{m}_k^T$  such that  $\|\hat{r}_k\|_2 \leq \varepsilon$ . Writing  $\hat{r}_k = e_k - A^T \hat{m}_k^T + \Delta \hat{r}_k$ , we have

$$\begin{aligned} \|e_k - A^T \hat{m}_k^T\|_2 &\leq \|\hat{r}_k\|_2 + \|\Delta \hat{r}_k\|_2 \\ &\leq \varepsilon + \tilde{\gamma}_n^f \|e_k\| + |A^T| \|\hat{m}_k^T\|_2 \\ &\leq 2\varepsilon, \end{aligned}$$

with which we can write the Frobenius norm bound

$$\|I - A^T \hat{M}^T\|_F \leq 2\sqrt{n}\varepsilon.$$

Note that assuming exact arithmetic, e.g., using  $u_f = 0$  in (3.2), the above bound becomes  $\|I - A^T M^T\|_F \leq \sqrt{n}\varepsilon$ , which is the same bound given by Grote and Huckle [20, Theorem 3.1]. At this point we can transpose to get the desired bound for the left preconditioned case and then convert to the desired infinity norm, giving

$$(3.5) \quad \|I - \widehat{M}A\|_\infty \leq 2n\varepsilon.$$

We note that from (3.5) we then also have an a priori bound on the distance from the computed  $\widehat{M}$  to the true inverse of  $A$ ,

$$(3.6) \quad \|\widehat{M} - A^{-1}\|_\infty \leq 2n\varepsilon\|A^{-1}\|_\infty.$$

An important conclusion that we can draw from this analysis, in particular from the fact that (3.5) is guaranteed as long as (3.4) holds, is that there is *no advantage* to using a higher precision in computing the SPAI preconditioner beyond that dictated by  $u_f \approx n\varepsilon \text{cond}_2^{-1}(A^T)$ . Using higher precision will have very little effect, since we will end up with a preconditioner of similar quality. We will demonstrate this observation in Section 4 below. Note that this is in contrast to the case of using full LU factorization, where the quality of the factors scales with the precision used.

Intuitively, however, we may think that using higher precision for  $u_f$  might result in an  $\widehat{M}$  with fewer (more accurate) nonzeros than an  $\widehat{M}$  computed in lower precision. This can be the case, but not necessarily. We demonstrate this in Figure 3.1 for the matrices **saylr1** (left plot) and **steam3** (right plot) from SuiteSparse [14], where we plot the number of nonzeros in the resulting  $\widehat{M}$  computed using the SPAI algorithm (Algorithm 2.1) in single precision (blue squares) and double precision (red circles) for various  $\varepsilon$  values. As we can see, for **saylr1**, there is very little difference between single and double precision in the resulting size of  $\widehat{M}$ ; if anything, single precision results in an  $\widehat{M}$  with slightly fewer nonzeros. For the matrix **steam3**, we do see this phenomenon, i.e.,  $\widehat{M}$  computed in double precision has fewer nonzeros than the  $\widehat{M}$  computed in single precision. Note that for both matrices, these choices of  $\varepsilon$  satisfy (3.4) for both single and double precision. We will explore further examples in Section 4.3.

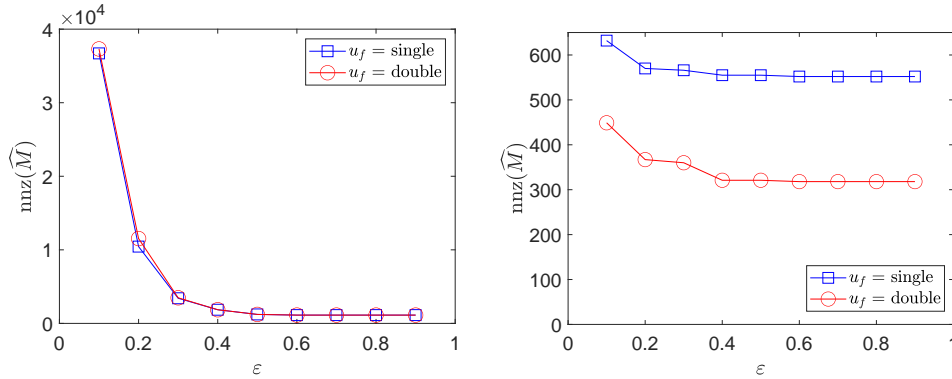


Fig. 3.1: Number of nonzeros in the computed sparse approximate inverse preconditioner  $\widehat{M}$  when  $\widehat{M}$  is computed in single precision (blue squares) and double precision (red circles), for the matrices **saylr1** (left) and **steam3** (right), for various choices of  $\varepsilon$ .

We will now briefly address the second question, which asks what we can say about the quality of  $\widehat{M}$  computed in precision  $u_f$  if we fix the sparsity structure of  $\widehat{M}$  to be the same sparsity structure we would obtain for the exact precision case with stopping criterion  $\|r_k\|_2 \leq \varepsilon$ . In this case, from (3.2), we have

$$(3.7) \quad \|e_k - A^T \widehat{m}_k^T\|_2 \leq n^2 \tilde{\gamma}_n^f \|e_k\| + |A^T| \|\widehat{m}_k^T\|_2 + (1 + n^2 \tilde{\gamma}_n^f \text{cond}_2(A)) \varepsilon + O(u_f^2).$$

From this, we can obtain

$$(3.8) \quad \|I - \widehat{M}A\|_\infty \leq n(\varepsilon + n^{5/2} \tilde{\gamma}_n^f \kappa_\infty(A)),$$

where we again note that if  $u_f = 0$  this reduces to the bound given by Grote and Huckle [20, Theorem 3.1]. This indicates that if  $\kappa_\infty(A)$  is much larger than  $\varepsilon u_f^{-1}$ , the computed  $\widehat{M}$  with the same sparsity structure as the exact  $M$  can be of much lower quality. We again stress that we will use the bound (3.5) rather than (3.8) in the remainder of this work, since in our experiments we will use the stopping criterion  $\|\widehat{r}_k\|_2 \leq \varepsilon$ . In practice, if a maximum sparsity structure is specified and the corresponding value of  $\varepsilon$  such that for all  $k$ ,  $\|r_k\|_2 \leq \varepsilon$  is known, then the above result may be useful.

**3.1. Standard iterative refinement with SPAI.** For illustrative purposes, let's say we want to build an iterative refinement scheme that uses a sparse approximate inverse rather than an LU factorization as the solver. In standard iterative refinement, in each step, using working precision  $u$  we will solve  $Ad_i = \widehat{r}_i$  via

$$(3.9) \quad \widehat{d}_i = fl(\widehat{M}\widehat{r}_i) = \widehat{M}\widehat{r}_i + \Delta d_i, \quad |\Delta d_i| \leq \gamma_n |\widehat{M}| |\widehat{r}_i|.$$

Then

$$\widehat{d}_i - d_i = \widehat{M}\widehat{r}_i + \Delta d_i - d_i = \widehat{M}Ad_i + \Delta d_i - d_i = (\widehat{M}A - I)d_i + \Delta d_i,$$

which using (3.5) along with (3.6) gives the bound

$$\frac{\|\widehat{d}_i - d_i\|_\infty}{\|d_i\|_\infty} \leq (1 + \tilde{\gamma}_n \kappa_\infty(A)) 2n\varepsilon.$$

Given (3.4) and assuming  $u \leq u_f$ , we expect the right hand side in this bound to be  $O(n)\varepsilon$ . In order for the iterative refinement scheme to converge, it is necessary that there is some degree of relative accuracy in the solve, meaning that, combined with condition (3.4), we require

$$(3.10) \quad nu_f \text{cond}_2(A^T) \lesssim n\varepsilon \lesssim 1.$$

In order for such a refinement scheme to converge, we therefore need two constraints to be met. First, we need  $u_f \text{cond}_2(A^T) \leq \varepsilon$  from (3.4) in order to guarantee that the SPAI algorithm completes. Second, we need  $O(n)\varepsilon < 1$ , which means that the computed approximate inverse sufficiently approximates the inverse of  $A$ . Given that typical values of  $\varepsilon$  range between 0.1 and 0.5, the requirement that  $n\varepsilon \lesssim 1$  is perhaps the more worrisome constraint. For even  $n = 100$ , say, we then need  $\varepsilon < 0.01$ . This means that the approximate inverse may be quite expensive to compute in some cases (perhaps requiring a least squares solve with the entirety of  $A$  for each column), and may not end up being all that sparse. Further, this constraint on  $\varepsilon$  then means

that if we use, say, half precision, we must have  $\text{cond}_2(A^T) \leq \varepsilon u_f^{-1} \approx 20$ . Again we note that the factor of  $n$  may be an overestimate in practice, so the approach may work even in the case that  $n\varepsilon > 1$ .

While this may work for some problems, this is obviously not a good idea in general; sparse approximate inverses were designed to be preconditioners rather than stand-alone solve techniques. When we throw away information in constructing the sparse approximate inverse, this information will not be recovered. A much more fruitful approach will be to use the SPAI matrix  $\widehat{M}$  as a left preconditioner within GMRES-based iterative refinement, which we now explore.

**3.2. GMRES-based iterative refinement with SPAI.** Our goal is now to bound the relative error in the correction solve when the solver is GMRES left-preconditioned by the approximate inverse  $\widehat{M}$ . For clarity, we present this variant, which we call SPAI-GMRES-IR, in Algorithm 3.1. We follow and heavily rely on the analysis of [10]. Here we will assume that the preconditioner and preconditioned coefficient matrix are applied to a vector in double the working precision,  $u^2$ . To determine constraints for the case that a single precision is used throughout GMRES, one could similarly follow the analysis in [3].

---

**Algorithm 3.1** GMRES-based Iterative Refinement with SPAI Preconditioning (SPAI-GMRES-IR)

---

**Input:**  $n \times n$  nonsingular matrix  $A$  and length- $n$  right-hand side vector  $b$ , maximum number of refinement steps  $i_{max}$ , GMRES convergence tolerance  $\tau$ , SPAI parameter  $\varepsilon$ .

**Output:** Approximate solution  $x_{i+1}$  to  $Ax = b$ .

- 1: Compute sparse approximate inverse  $M$  of  $A$  in precision  $u_f$  with parameter  $\varepsilon$  using Algorithm 2.1.
  - 2: Compute  $x_0 = Mb$  in precision  $u_f$ ; store  $x_0$  in precision  $u$ .
  - 3: **for**  $i = 0 : i_{max} - 1$  **do**
  - 4:   Compute  $r_i = b - Ax_i$  in precision  $u_r$ ; store in precision  $u$ .
  - 5:   Solve  $MA d_i = M r_i$  via left-preconditioned GMRES in working precision  $u$ , with matrix-vector products with  $M$  and  $\tilde{A} = MA$  computed in precision  $u^2$ ; store  $d_i$  in precision  $u$ .
  - 6:   Update  $x_{i+1} = x_i + d_i$  in precision  $u$ .
  - 7: **end for**
- 

We first want to bound  $\kappa_\infty(\tilde{A})$ , where  $\tilde{A} = \widehat{M}A$ . We stress that the condition number of the preconditioned matrix will not tell us anything about the convergence rate of GMRES (see [19]); here we will use it to bound the relative error after we obtain a backward error result for the preconditioned system. We can write

$$\begin{aligned}
 \tilde{A} &= \widehat{M}A = I - (I - \widehat{M}A), \\
 \tilde{A}^{-1} &= A^{-1}\widehat{M}^{-1} = (I - (I - \widehat{M}A))^{-1} \\
 &\approx I + (I - \widehat{M}A).
 \end{aligned}
 \tag{3.11}$$

Thus using (3.5), we have

$$\begin{aligned}
 \|\tilde{A}\|_\infty &\leq 1 + 2n\varepsilon, \\
 \|\tilde{A}^{-1}\|_\infty &\lesssim 1 + 2n\varepsilon,
 \end{aligned}$$

which gives

$$(3.12) \quad \kappa_\infty(\tilde{A}) \lesssim (1 + 2n\varepsilon)^2.$$

We note that this should not be taken as an upper bound but rather as a rough estimate, since for practical problem sizes,  $2n\varepsilon$  will likely be greater than 1, and our dropping of higher order terms in the Taylor expansion to get (3.11) may be dubious. Although (3.12) is not strictly an upper bound, we note that the growth of  $\kappa_\infty(\tilde{A})$  does generally follow this bound asymptotically. In Figure 3.2, we plot the condition number  $\kappa_\infty(\tilde{A})$  versus  $\varepsilon$  for two matrices from SuiteSparse [14], **saylr1** (Fig. 3.2a) and **steam3** (Fig. 3.2b), where the sparse approximate inverses are computed in single precision (blue squares) and double precision (red circles). We additionally plot  $(1 + 2n\varepsilon)^2$ , the estimate in (3.12), demonstrating that (3.12) well describes the resulting condition number of the preconditioned coefficient matrix. We again note that there is little difference between single and double precision, since we expect preconditioner quality to depend on  $\varepsilon$  rather than  $u_f$  as long as (3.4) is satisfied.

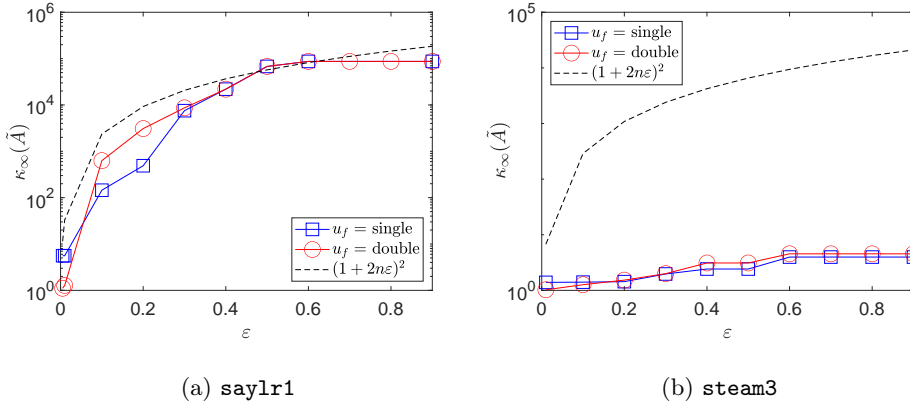


Fig. 3.2:  $\kappa_\infty(\tilde{A})$  versus  $\varepsilon$  for matrices **saylr1** (left) and **steam3** (right) for SPAI preconditioners computed in single (blue squares) and double (red circles), compared with the rough bound (3.12).

Now we turn our attention to the application of the preconditioner to the right-hand side  $\hat{r}_i$ . Let the (exact) preconditioned right-hand side be  $z_i = \widehat{M}\hat{r}_i$ . Assuming we apply  $\widehat{M}$  to  $\hat{r}_i$  in double the working precision, we have

$$\begin{aligned} \hat{z}_i &= (\widehat{M} + \Delta M)\hat{r}_i, & |\Delta M| &\leq \bar{\gamma}_n |\widehat{M}|, \\ &= z_i + \Delta M \widehat{M}^{-1} z_i, \end{aligned}$$

where  $\bar{\gamma}_k = ku^2/(1 - ku^2)$ . We then have the bound

$$(3.13) \quad \|\hat{z}_i - z_i\|_\infty \leq \bar{\gamma}_n \|\widehat{M}\| \|\widehat{M}^{-1}\|_\infty \|z_i\|_\infty.$$

Assuming that  $\kappa_\infty(\widehat{M}) \approx \kappa_\infty(A) \lesssim u^{-1}$ , then we expect  $\|\hat{z}_i - z_i\|_\infty \leq \bar{\gamma}_n \|z_i\|_\infty$ .

Following [10], we now seek to bound the error in applying  $\widehat{M}A$  to a vector  $\widehat{v}_j$  in iteration  $j$  of the GMRES algorithm. We compute this via

$$\begin{aligned}(A + \delta A)\widehat{v}_j &= \widehat{w}_j, & |\Delta A| &\leq \bar{\gamma}_n |A| \\ (\widehat{M} + \Delta \widehat{M})\widehat{w}_j &= \widehat{y}_j, & |\Delta M| &\leq \bar{\gamma}_n |\widehat{M}|.\end{aligned}$$

Then we can write the computed vector  $\widehat{y}_j$  as

$$\widehat{y}_j = (\widehat{M} + \Delta M)(A + \Delta A)\widehat{v}_j = (\widehat{M}A + \Delta MA + \widehat{M}\Delta A)\widehat{v}_j = (\tilde{A} + \Delta \tilde{A}')\widehat{v}_j,$$

where

$$\begin{aligned}\Delta \tilde{A}' &= \Delta MA + \widehat{M}\Delta A \\ &= \Delta M\widehat{M}^{-1}\widehat{M}A + \widehat{M}AA^{-1}\Delta A \\ &= \Delta M\widehat{M}^{-1}\tilde{A} + \tilde{A}A^{-1}\Delta A,\end{aligned}$$

for which we can write the bound

$$\begin{aligned}\|\Delta \tilde{A}'\|_F &\leq \bar{\gamma}_n (\|\widehat{M}\|\|\widehat{M}^{-1}\|_F + \|A^{-1}\|_F\|A\|_F)\|\tilde{A}\|_F \\ &\leq \bar{\gamma}_n (\kappa_F(\widehat{M}) + \kappa_F(A))\|\tilde{A}\|_F.\end{aligned}$$

Then as long as  $\kappa_F(\widehat{M}) \approx \kappa_F(A) \lesssim u^{-1}$ , we will have

$$\|\Delta \tilde{A}'\|_F \leq \bar{\gamma}_n \|\tilde{A}\|_F.$$

Following through the analysis in [10], the above bound implies that for some iteration  $k \leq n$ , the left-preconditioned MGS-GMRES algorithm will produce an approximate solution  $\widehat{d}_i$  for which

$$(3.14) \quad (\tilde{A} + \Delta \tilde{A}')\widehat{d}_i = \widehat{z}_i + \Delta \widehat{z}_i, \quad \|\Delta \tilde{A}'\|_F \leq \bar{\gamma}_{kn} \|\tilde{A}\|_F, \quad \|\Delta \widehat{z}_i\|_2 \leq \bar{\gamma}_{kn} \|\widehat{z}_i\|_2.$$

Then together with (3.13), we can bound the normwise relative backward error by

$$\frac{\|z_i - \tilde{A}\widehat{d}_i\|_\infty}{\|\tilde{A}\|_\infty \|\widehat{d}_i\|_\infty + \|z_i\|_\infty} \lesssim n\bar{\gamma}_{kn},$$

which gives the relative forward error bound

$$\frac{\|\widehat{d}_i - d_i\|_\infty}{\|d_i\|_\infty} \lesssim n\bar{\gamma}_{kn}\kappa_\infty(\tilde{A}).$$

Using the estimate in (3.12), we can thus give the rough bound

$$(3.15) \quad \frac{\|\widehat{d}_i - d_i\|_\infty}{\|d_i\|_\infty} \lesssim n\bar{\gamma}_{kn}(1 + 2n\varepsilon)^2.$$

Combining this with (3.4), we thus must have roughly

$$2nu_f \text{cond}_2(A^T) \lesssim 2n\varepsilon \lesssim u^{-1/2}$$

in order to guarantee that both that the SPAI algorithm will complete and that the GMRES-based iterative refinement scheme will converge.

Note that from (3.15), we have that for SPAI-GMRES-IR, the quantity  $u_s \|E_i\|_\infty$  in (2.1) is on the order  $uf(n)(1+n\varepsilon)^2$ , for  $f(n) = O(n^2)$ , and by (3.14), the quantities  $c_1$  and  $c_2$  in (2.2) and  $G_i$  in (2.3) will be the same as for GMRES-IR.

Notice that in contrast to the standard iterative refinement case, here we need  $n\varepsilon \lesssim u^{-1/2}$ , which is much less stringent than  $n\varepsilon \lesssim 1$ . This makes sense, since the quality of the approximate inverse matters much less since we are only using it as a preconditioner.

Comparing the expected behavior of SPAI-GMRES-IR and GMRES-IR with full LU factorization, we expect that convergence for GMRES with the SPAI preconditioner will in general be slower than GMRES using the full LU factors, at least when we assume common choices of  $\varepsilon$ . The tradeoff is that the SPAI preconditioner will hopefully be much sparser and less expensive to apply than triangular solves with the full LU factors. As this behavior and the resulting tradeoffs will be strongly problem dependent, we turn to numerical experiments to demonstrate the potential benefits of SPAI-GMRES-IR.

**4. Numerical Experiments.** We now turn to an experimental evaluation of the numerical behavior of SPAI-GMRES-IR, in particular in comparison to GMRES-IR with full LU factorization (which in this section we refer to as LU-GMRES-IR). Our experiments are performed in MATLAB R2021a. In these experiments we use four precisions. For half precision, we use the `chop` library available at <https://github.com/higham/chop>. For quadruple precision, we use the Advanpix Multiprecision Computing Toolbox [33]. For single and double precision we use the built-in MATLAB datatypes. The code used to generate plots in this work can be found at <https://github.com/Noaman67khan/SPAI-GMRES-IR>.

The matrices tested come from the SuiteSparse Matrix Collection [14]. We list tested matrices and their relevant properties in Table 4.1. The right-hand sides are set to the vector of ones in all cases. For single working precision, we use  $10^{-4}$  as the convergence tolerance for GMRES, and for double working precision we use  $10^{-4}$ . In all cases, we set the initial sparsity pattern for SPAI to be the pattern of  $A^T$ , which guarantees an  $M$  with nonzero columns [34, Theorem 3.1].

For each linear system and given combination of precisions, we run SPAI-GMRES-IR with various values of  $\varepsilon$  (top 2 plots in each figure), GMRES-IR with full LU factors as preconditioners (bottom left plots in each figure), and GMRES-IR but with no preconditioning (bottom right plots in each figure). The red, blue, and green lines in the figures show the behavior of the forward error ‘ferr’ (red), the normwise relative backward error ‘nbe’ (blue), and the componentwise relative backward error ‘cbe’ (green) for the given iterative refinement scheme. The dotted black line shows the level of the working precision  $u$ . The number above the marker at  $i$  on the x-axis in each plot display the number of GMRES iterations in refinement step  $i$ . The condition numbers of the preconditioned systems are shown in the titles of each figure.

Each figure is accompanied by a table which, for each setup, gives the size of the preconditioner in terms of number of nonzeros as well as information about the number of GMRES-IR refinement steps and GMRES iterations per refinement step. For LU factorization, the size is given as  $nnz(L + U)$ . For the final column in the tables, the first number gives the total number of GMRES iterations summed over all refinement steps, and the following tuple gives in position  $i$  the number of GMRES iterations in refinement step  $i$ . For the SPAI preconditioners, we also list the values of  $\alpha$  and  $\beta$  used to generate  $M$ ; see Algorithm 2.1. We note that some tables give additional experiments with SPAI preconditioners for values of  $\varepsilon$  beyond what is shown in the



Table 4.1: Matrices used in experiments along with their properties. All matrices come from the SuiteSparse collection [14].

Name	$n$	$nnz$	$\kappa_\infty(A)$	$\text{cond}_2(A^T)$
<b>arc130</b>	130	1037	$1.2 \cdot 10^{12}$	$4.8 \cdot 10^5$
<b>bfw782a</b>	782	7514	$6.8 \cdot 10^3$	$1.3 \cdot 10^3$
<b>cake5</b>	37	233	$2.9 \cdot 10^1$	$7.5 \cdot 10^0$
<b>cdde4</b>	961	4681	$1.7 \cdot 10^2$	$7.7 \cdot 10^1$
<b>fs_541_2</b>	541	4282	$9.4 \cdot 10^9$	$2.4 \cdot 10^6$
<b>hor_131</b>	434	4182	$1.5 \cdot 10^5$	$3.3 \cdot 10^3$
<b>jpwh_991</b>	991	6027	$3.5 \cdot 10^2$	$1.0 \cdot 10^2$
<b>lms_511</b>	511	2796	$1.0 \cdot 10^{16}$	$6.8 \cdot 10^5$
<b>saylr1</b>	238	1128	$1.6 \cdot 10^9$	$5.2 \cdot 10^5$
<b>steam1</b>	240	2248	$3.1 \cdot 10^7$	$2.8 \cdot 10^3$
<b>steam3</b>	80	314	$7.6 \cdot 10^{10}$	$5.6 \cdot 10^3$

plots.

The best case scenario is that SPAI preconditioning produces a preconditioner that is much sparser than the full LU factorization and requires only a small number of additional refinement steps compared to GMRES-IR with full LU preconditioning. For many (but not all) examples, this behavior is observed. In the Section 4.1, we give examples using precisions  $(u_f, u, u_r) = (\text{single}, \text{double}, \text{quad})$  and in Section 4.2, we use  $(u_f, u, u_r) = (\text{half}, \text{single}, \text{double})$ . Finally, in Section 4.3, we redo a few of the experiments using  $(u_f, u, u_r) = (\text{half}, \text{single}, \text{double})$  but now using  $(u_f, u, u_r) = (\text{single}, \text{single}, \text{double})$ . These results demonstrate that there is often not a significant advantage, either in terms of the size of the preconditioner or the total number of GMRES iterations, to using  $u_f$  higher than that dictated by the constraint (3.4). That is, the resulting SPAI preconditioner will satisfy (3.5) regardless of whether half or single precision is used, and thus do not expect much difference in the behavior of the iterative refinement process.

**4.1. Experiments with  $(u_f, u, u_r) = (\text{single}, \text{double}, \text{quad})$ .** As mentioned above, we show both examples where SPAI-GMRES-IR exhibits the desired behavior, that is, SPAI-GMRES-IR performs almost as well as GMRES-IR with LU preconditioning in terms of total number of GMRES iterations and uses a much sparser preconditioner, as well as examples where SPAI-GMRES-IR is not as effective.

For **steam1** (Figure 4.1, Table 4.2), the full LU factors contain 21,657 nonzeros, almost 10 times the number of nonzeros in  $A$ . Both choices of  $\varepsilon = 0.1$  and  $\varepsilon = 0.2$  result in a very sparse approximate inverse  $M$  with 2,248 nonzeros, the same number of nonzeros as  $A$  (which is as sparse as our algorithm will allow, since we start with the initial sparsity structure of  $A^T$ ). Whereas LU-GMRES-IR requires only 3 GMRES iterations across 2 refinement steps, SPAI requires 9 total GMRES iterations across 3 refinement steps, which is a minimal increase relative to the cost of GMRES-IR without preconditioning (here 672 total GMRES iterations).

The story for **arc130** (Figure 4.2, Table 4.3) is similar; SPAI results in a preconditioner with almost  $8\times$  fewer nonzeros, but requires only up to a factor of  $5\times$  more GMRES iterations (2 for LU-GMRES-IR versus 9 or 10 with SPAI-GMRES-IR). For **steam3**, the results are slightly less impressive but still acceptable. Here,

using  $\varepsilon = 0.1$ , we obtain an SPAI preconditioner with half the nonzeros as the LU factors, with only 10 more GMRES iterations required. This is still a good rate of convergence relative to GMRES-IR with no preconditioning, which requires 205 total GMRES iterations, indicating that the SPAI preconditioner is still effective.

For `steam3` (Figure 4.3, Table 4.4), the number of GMRES iterations required is increased only slightly for SPAI-GMRES-IR relative to LU-GMRES-IR, but the decrease in the size of the preconditioner is not as significantly (about half the number of nonzeros for the two values of  $\varepsilon$  tested).

For the problem with matrix `saylr1` (Figure 4.4, Table 4.5), the behavior of SPAI-GMRES-IR is not terrible, but perhaps just not impressive. LU-GMRES-IR converges very quickly, whereas SPAI-GMRES-IR with both  $\varepsilon = 0.3$  and  $\varepsilon = 0.4$  requires a significant number of GMRES iterations to converge (only roughly half that of using no preconditioning). If  $\varepsilon$  is chosen much smaller, as 0.01, then the number of GMRES iterations significantly decreases, but the “sparse” approximate inverse is not very sparse at all (almost as dense as the full inverse of  $A$ ).

For `lms_511`, (Figure 4.5, Table 4.6), no choice of  $\varepsilon$  that we tested significantly reduced the size of the preconditioner while maintaining a reasonable GMRES convergence rate. For the choice  $\varepsilon = 0.2$ , the preconditioner already has more nonzeros than the LU factors (and with a worse GMRES convergence rate).

Finally, for `fs_541_2` (Figure 4.6, Table 4.7), although the SPAI preconditioners are much sparser than the full LU factors, they did not result in a reasonably significant convergence rate relative to the unpreconditioned case for any value of  $\varepsilon$  tested.

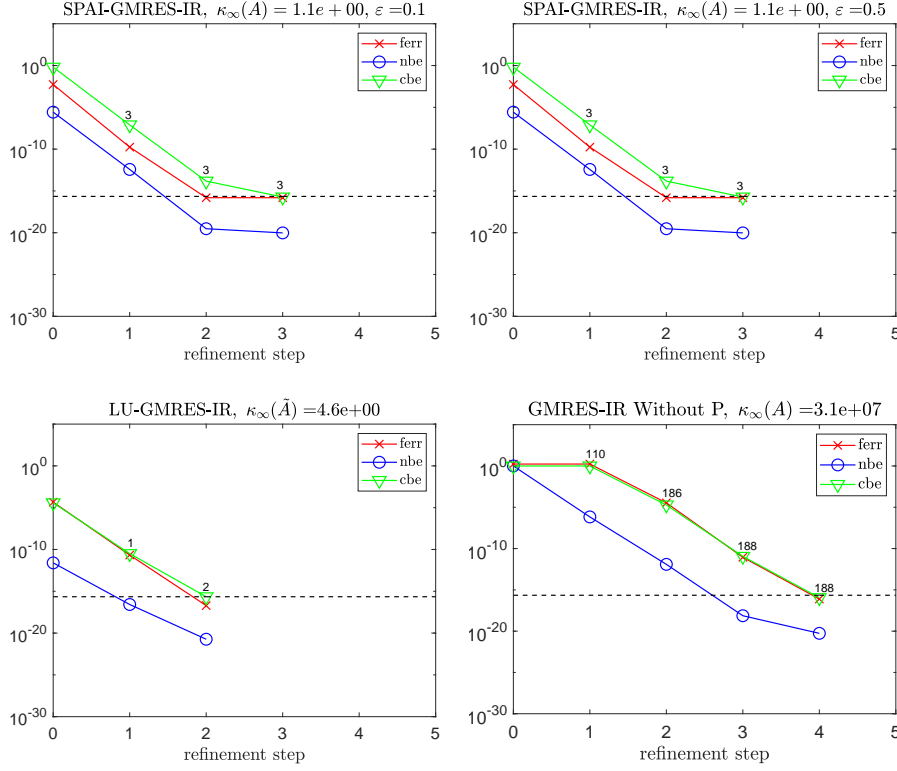


Fig. 4.1: **steam1** (S, D, Q). Convergence of the forward error (ferr), normwise backward error (nbe) and componentwise backward error (cbe) for iterative refinement on a problem with the matrix **steam1** using SPAI-GMRES-IR with  $\varepsilon = 0.1$  (top left) and  $\varepsilon = 0.5$  (top right), LU-GMRES-IR (bottom left), and GMRES-IR with no preconditioning (bottom right), using precisions  $(u_f, u, u_r) = (\text{single}, \text{double}, \text{quad})$ . Numbers on data markers give the number of GMRES iterations in the given refinement step.

Table 4.2: **steam1** (S, D, Q). Comparison of SPAI-GMRES-IR for different  $\varepsilon$  values with LU-GMRES-IR and GMRES-IR with no preconditioner for the matrix **steam1** using  $(u_f, u, u_r) = (\text{single}, \text{double}, \text{quad})$ . For this matrix,  $n = 240$ ,  $\text{nnz}(A) = 2248$ , and  $\text{nnz}(A^{-1}) = 57596$ .

Preconditioner	Precond. $\text{nnz}$	GMRES-IR steps/iterations
SPAI ( $\varepsilon = 0.1$ , $\alpha = 20$ , $\beta = 20$ )	2248	9(3, 3, 3)
SPAI ( $\varepsilon = 0.2$ , $\alpha = 20$ , $\beta = 20$ )	2248	9(3, 3, 3)
Full LU	21657	3(1, 2)
None	0	672(110, 186, 188, 188)

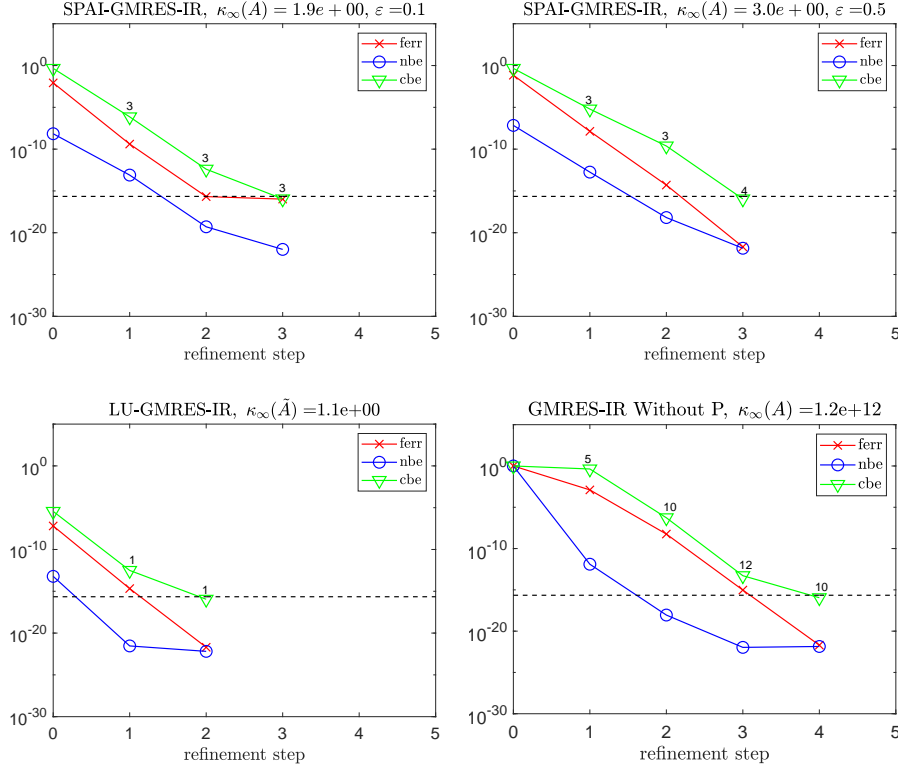


Fig. 4.2: `arc130` (S, D, Q). Convergence of the forward error (ferr), normwise backward error (nbe) and componentwise backward error (cbe) for iterative refinement on a problem with the matrix `arc130` using SPAI-GMRES-IR with  $\varepsilon = 0.1$  (top left) and  $\varepsilon = 0.5$  (top right), LU-GMRES-IR (bottom left), and GMRES-IR with no preconditioning (bottom right), using precisions  $(u_f, u, u_r) = (\text{single}, \text{double}, \text{quad})$ . Numbers on data markers give the number of GMRES iterations in the given refinement step.

Table 4.3: `arc130` (S, D, Q). Comparison of SPAI-GMRES-IR for different  $\varepsilon$  values with GMRES-IR with full LU and with no preconditioner for the matrix `arc130` using  $(u_f, u, u_r) = (\text{single}, \text{double}, \text{quad})$ . For this matrix,  $n = 130$ ,  $\text{nnz}(A) = 1037$ , and  $\text{nnz}(A^{-1}) = 10026$ .

Preconditioner	Precond. $\text{nnz}$	GMRES-IR steps/iterations
SPAI ( $\varepsilon = 0.1$ , $\alpha = 70$ , $\beta = 70$ )	1172	9(3, 3, 3)
SPAI ( $\varepsilon = 0.5$ , $\alpha = 70$ , $\beta = 70$ )	1141	10(3, 3, 4)
Full LU	9204	2(1, 1)
None	0	37(5, 10, 12, 10)

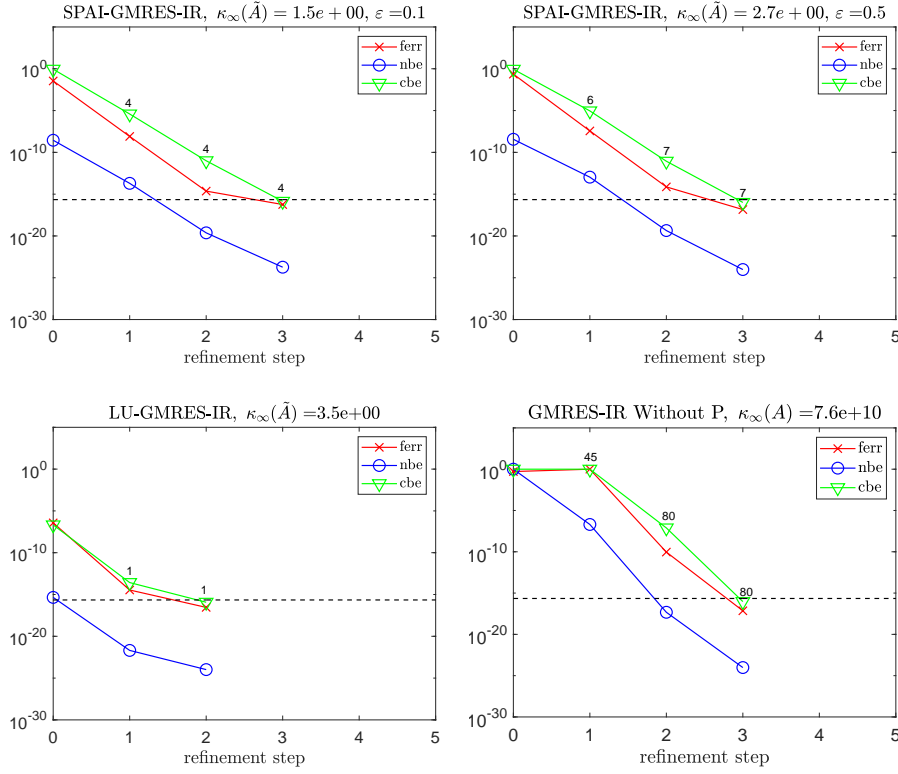


Fig. 4.3: **steam3** (S, D, Q). Convergence of the forward error (ferr), normwise backward error (nbe) and componentwise backward error (cbe) for iterative refinement on a problem with the matrix **steam3** using SPAI-GMRES-IR with  $\varepsilon = 0.1$  (top left) and  $\varepsilon = 0.5$  (top right), LU-GMRES-IR (bottom left), and GMRES-IR with no preconditioning (bottom right), using precisions  $(u_f, u, u_r) = (\text{single}, \text{double}, \text{quad})$ . Numbers on data markers give the number of GMRES iterations in the given refinement step.

Table 4.4: **steam3** (S, D, Q). Comparison of SPAI-GMRES-IR for different  $\varepsilon$  values with GMRES-IR with full LU and with no preconditioner for the matrix **steam3** using  $(u_f, u, u_r) = (\text{single}, \text{double}, \text{quad})$ . For this matrix,  $n = 80$ ,  $\text{nnz}(A) = 314$ , and  $\text{nnz}(A^{-1}) = 6315$ .

Preconditioner	Precond. $\text{nnz}$	GMRES-IR steps/iterations
SPAI ( $\varepsilon = 0.1$ , $\alpha = 10$ , $\beta = 10$ )	546	12(4, 4, 4)
SPAI ( $\varepsilon = 0.2$ , $\alpha = 20$ , $\beta = 20$ )	479	20(6, 7, 7)
Full LU	987	2(1, 1)
None	0	205(45, 80, 80)

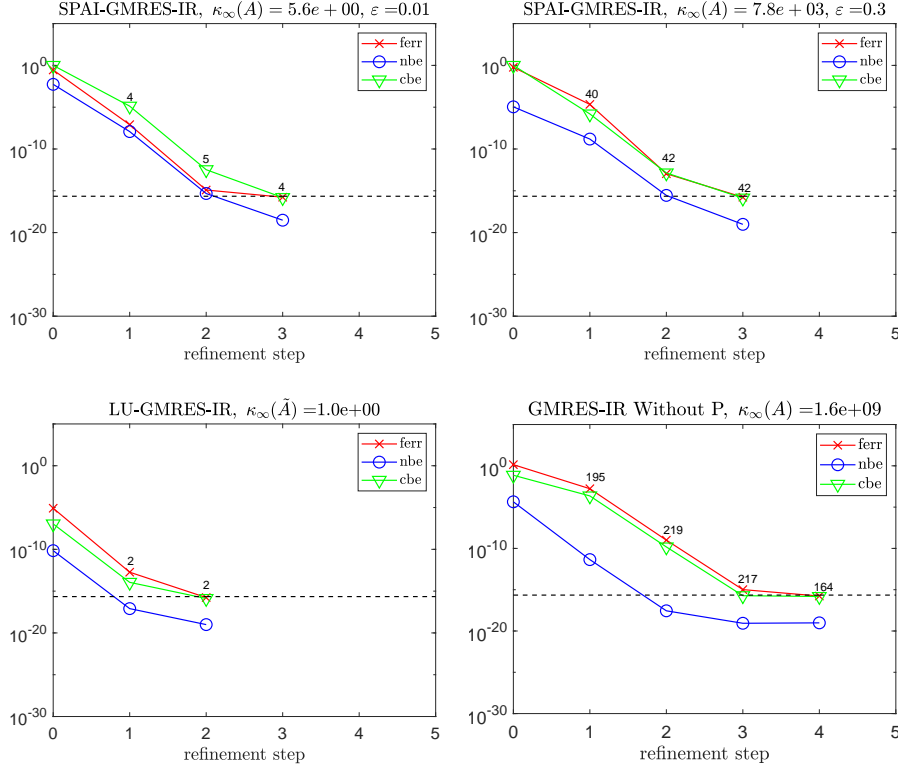


Fig. 4.4: **saylr1** (S, D, Q). Convergence of the forward error (ferr), normwise backward error (nbe) and componentwise backward error (cbe) for iterative refinement on a problem with the matrix **saylr1** using SPAI-GMRES-IR with  $\varepsilon = 0.01$  (top left) and  $\varepsilon = 0.3$  (top right), LU-GMRES-IR (bottom left), and GMRES-IR with no preconditioning (bottom right), using precisions  $(u_f, u, u_r) = (\text{single}, \text{double}, \text{quad})$ . Numbers on data markers give the number of GMRES iterations in the given refinement step.

Table 4.5: **saylr1** (S, D, Q). Comparison of SPAI-GMRES-IR for different  $\varepsilon$  values with GMRES-IR with full LU and with no preconditioner for the matrix **saylr1** using  $(u_f, u, u_r) = (\text{single}, \text{double}, \text{quad})$ . For this matrix,  $n = 238$ ,  $\text{nnz}(A) = 1128$ , and  $\text{nnz}(A^{-1}) = 56644$ .

Preconditioner	Precond. $\text{nnz}$	GMRES-IR steps/iterations
SPAI ( $\varepsilon = 0.01$ , $\alpha = 50$ , $\beta = 50$ )	52843	13(4, 5, 4)
SPAI ( $\varepsilon = 0.3$ , $\alpha = 20$ , $\beta = 20$ )	3418	124(40, 42, 42)
SPAI ( $\varepsilon = 0.4$ , $\alpha = 20$ , $\beta = 20$ )	1856	201(65, 67, 69)
Full LU	6548	4(2,2)
None	0	394(195, 219, 217, 164)

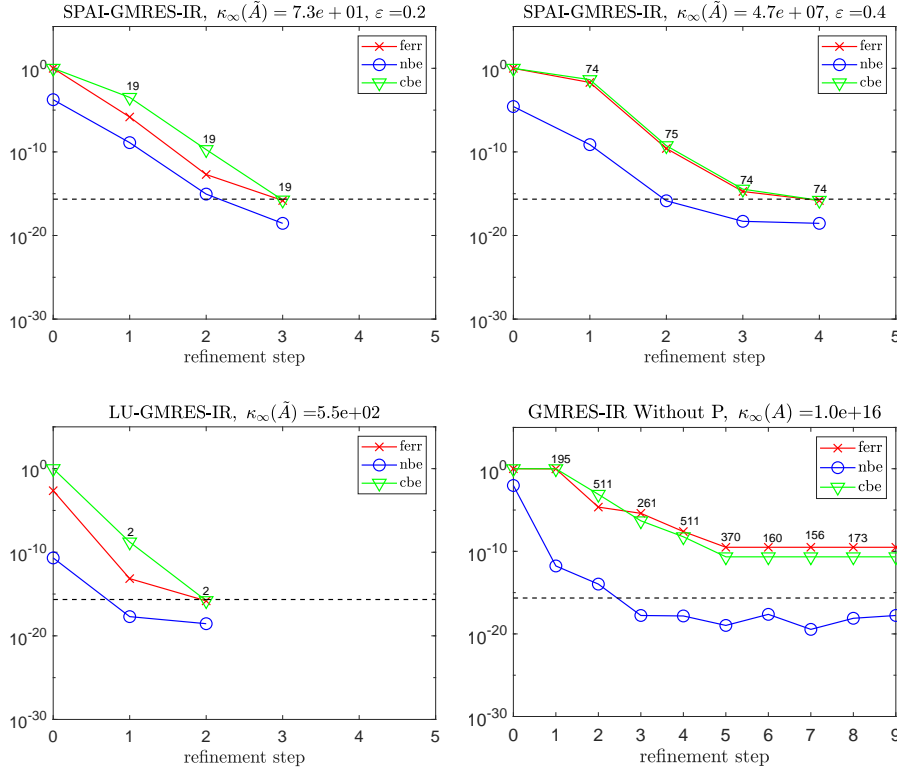


Fig. 4.5: **1ns\_511** (S, D, Q). Convergence of the forward error (ferr), normwise backward error (nbe) and componentwise backward error (cbe) for iterative refinement on a problem with the matrix **1ns\_511** using SPAI-GMRES-IR with  $\varepsilon = 0.2$  (top left) and  $\varepsilon = 0.4$  (top right), LU-GMRES-IR (bottom left), and GMRES-IR with no preconditioning (bottom right), using precisions  $(u_f, u, u_r) = (\text{single}, \text{double}, \text{quad})$ . Numbers on data markers give the number of GMRES iterations in the given refinement step.

Table 4.6: **1ns\_511** (S, D, Q). Comparison of SPAI-GMRES-IR for different  $\varepsilon$  values with GMRES-IR with full LU and with no preconditioner for the matrix **1ns\_511** using  $(u_f, u, u_r) = (\text{single}, \text{double}, \text{quad})$ . For this matrix,  $n = 511$ ,  $nnz(A) = 2796$ , and  $nnz(A^{-1}) = 225212$ .

Preconditioner	Precond. $nnz$	GMRES-IR steps/iterations
SPAI ( $\varepsilon = 0.2$ , $\alpha = 70$ , $\beta = 70$ )	71615	57(19, 19, 19)
SPAI ( $\varepsilon = 0.4$ , $\alpha = 70$ , $\beta = 70$ )	30301	297 (74, 75, 74, 74)
Full LU	46204	4(2, 2)
None	0	3432(195, 511, 261, 511, 370, 160, 156, 173, 150, 159, 150, 155, 158, 165, 158)



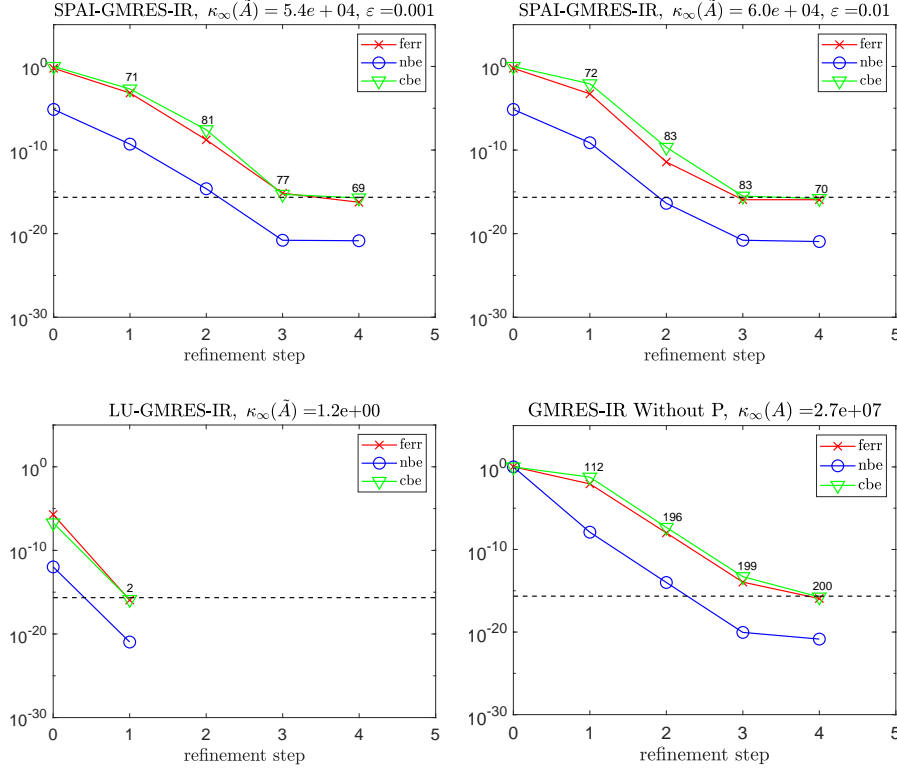


Fig. 4.6: **fs\_541\_2** (S, D, Q). Convergence of the forward error (ferr), normwise backward error (nbe) and componentwise backward error (cbe) for iterative refinement on a problem with the matrix **fs\_541\_2** using SPAI-GMRES-IR with  $\varepsilon = 0.001$  (top left) and  $\varepsilon = 0.01$  (top right), LU-GMRES-IR (bottom left), and GMRES-IR with no preconditioning (bottom right), using precisions  $(u_f, u, u_r) = (\text{single}, \text{double}, \text{quad})$ . Numbers on data markers give the number of GMRES iterations in the given refinement step.

Table 4.7: **fs\_541\_2** (S, D, Q). Comparison of SPAI-GMRES-IR for different  $\varepsilon$  values with GMRES-IR with full LU and with no preconditioner for the matrix **fs\_541\_2** using  $(u_f, u, u_r) = (\text{single}, \text{double}, \text{quad})$ . For this matrix,  $n = 541$ ,  $\text{nnz}(A) = 4282$ , and  $\text{nnz}(A^{-1}) = 292141$ .

Preconditioner	Precond. $\text{nnz}$	GMRES-IR steps/iterations
SPAI ( $\varepsilon = 0.001$ , $\alpha = 30$ , $\beta = 30$ )	50724	298(71, 81, 77, 69)
SPAI ( $\varepsilon = 0.01$ , $\alpha = 30$ , $\beta = 30$ )	31157	308(72, 83, 83, 70)
SPAI ( $\varepsilon = 0.1$ , $\alpha = 30$ , $\beta = 30$ )	18767	364(88, 95, 92, 89)
Full LU	117046	2(2)
None	0	707(112, 196, 199, 200)

**4.2. Experiments with  $(u_f, u, u_r) = (\text{half}, \text{single}, \text{double})$ .** We now turn to examples using precisions  $(u_f, u, u_r) = (\text{half}, \text{single}, \text{double})$ . We again note that we have limited ourselves to examples where the use of half precision does not cause over/underflow in the SPAI construction and that the development of matrix scaling techniques for this case are the subject of future work.

For **bfw782a** (Figure 4.7, Table 4.8), SPAI-GMRES-IR with  $\varepsilon = 0.2$  performs very well relative to LU-GMRES-IR. Here the SPAI preconditioner has more than  $12\times$  fewer nonzeros than the LU factors and requires about  $9\times$  more GMRES iterations total. This is still a good convergence rate relative to the unpreconditioned case. With  $\varepsilon = 0.5$ , the preconditioner is much sparser, with  $nnz(M)$  comparable to  $nnz(A)$ . The number of total GMRES iterations required, however, increases very significantly, although this is still  $3.5\times$  fewer iterations than the unpreconditioned case. This shows the sensitivity of SPAI-GMRES-IR to the particular choice of  $\varepsilon$ , which is highly problem-dependent.

For **hor\_131** (Figure 4.8, Table 4.9), both  $\varepsilon = 0.3$  and  $\varepsilon = 0.5$  result in decent behavior for SPAI-GMRES-IR, with different tradeoff points. Using  $\varepsilon = 0.5$  gives a preconditioner that has about  $10\times$  fewer nonzeros than the full LU factors, with an increase of 108 GMRES iterations total. Note that in this case SPAI-GMRES-IR still requires  $20\times$  fewer GMRES iterations than the case with no preconditioning.

The story is largely the same for the matrices **jpwh\_991** (Figure 4.9, Table 4.10) and **cdde4** (Figure 4.10, Table 4.11). For **jpwh\_991**, both choices of  $\varepsilon$  in SPAI-GMRES-IR result in a sparser preconditioner compared to the full LU factors, and still give a good reduction in the total number of GMRES iterations versus the unpreconditioned case. For **cdde4**, notice that the choice  $\varepsilon = 0.1$  results in a preconditioner that has more nonzeros than the LU factors, and despite this, more GMRES iterations are required. Again this emphasizes that the choice of  $\varepsilon$  is critical in SPAI-GMRES-IR.

For the matrix **gre\_115** (Figure 4.11, Table 4.12), choices of  $\varepsilon \leq 0.2$  resulted in a preconditioner that was nearly as dense or denser and less effective than the full LU factorization. For  $\varepsilon = 0.5$ , the SPAI preconditioner was significantly sparser than the LU factors, but SPAI-GMRES-IR required almost  $30\times$  more GMRES iterations than LU-GMRES-IR.

For the matrix **cage5** (Figure 4.12, Table 4.13), SPAI-GMRES-IR performs reasonably well relative to LU-GMRES-IR, but the results are perhaps not as impressive as the other cases.

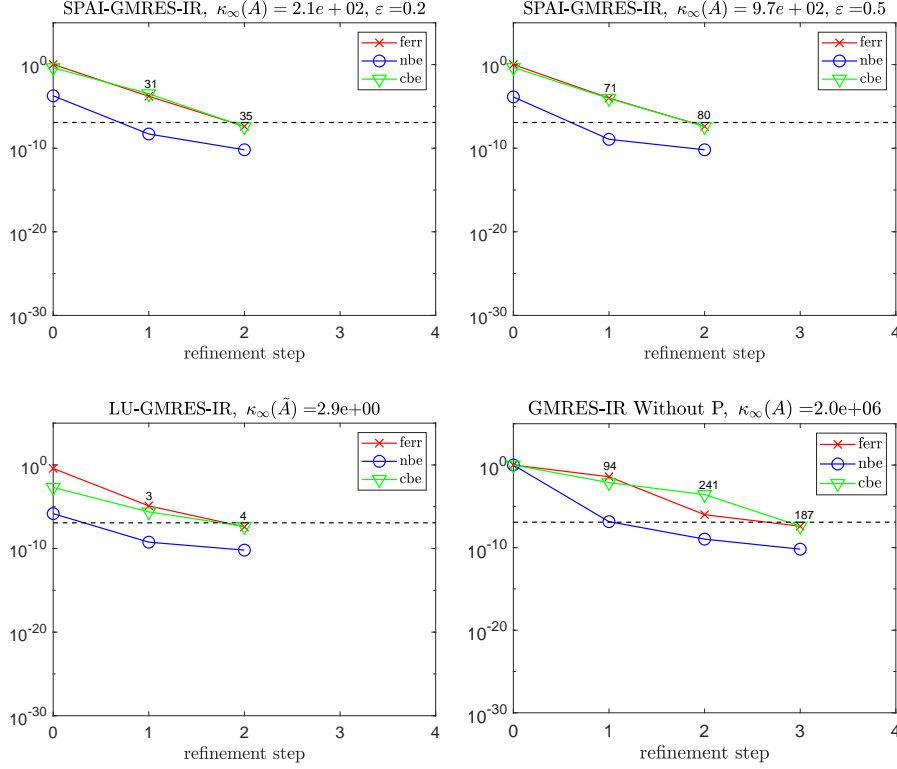


Fig. 4.7: **bfwa782** (H, S, D). Convergence of the forward error (ferr), normwise backward error (nbe) and componentwise backward error (cbe) for iterative refinement on a problem with the matrix **bfwa782** using SPAI-GMRES-IR with  $\varepsilon = 0.2$  (top left) and  $\varepsilon = 0.5$  (top right), LU-GMRES-IR (bottom left), and GMRES-IR with no preconditioning (bottom right), using precisions  $(u_f, u, u_r) = (\text{half}, \text{single}, \text{double})$ . Numbers on data markers give the number of GMRES iterations in the given refinement step.

Table 4.8: **bfwa782** (H, S, D). Comparison of SPAI-GMRES-IR for different  $\varepsilon$  values with GMRES-IR with full LU and with no preconditioner for the matrix **bfwa782** using  $(u_f, u, u_r) = (\text{half}, \text{single}, \text{double})$ . For this matrix,  $n = 782$ ,  $\text{nnz}(A) = 7514$ , and  $\text{nnz}(A^{-1}) = 458839$ .

Preconditioner	Precond. $\text{nnz}$	GMRES-IR steps/iterations
SPAI ( $\varepsilon = 0.2$ , $\alpha = 70$ , $\beta = 70$ )	28077	66(31, 35)
SPAI ( $\varepsilon = 0.5$ , $\alpha = 70$ , $\beta = 70$ )	7528	151(71, 80)
Full LU	347828	7(3,4)
None	0	522(94, 241, 187)

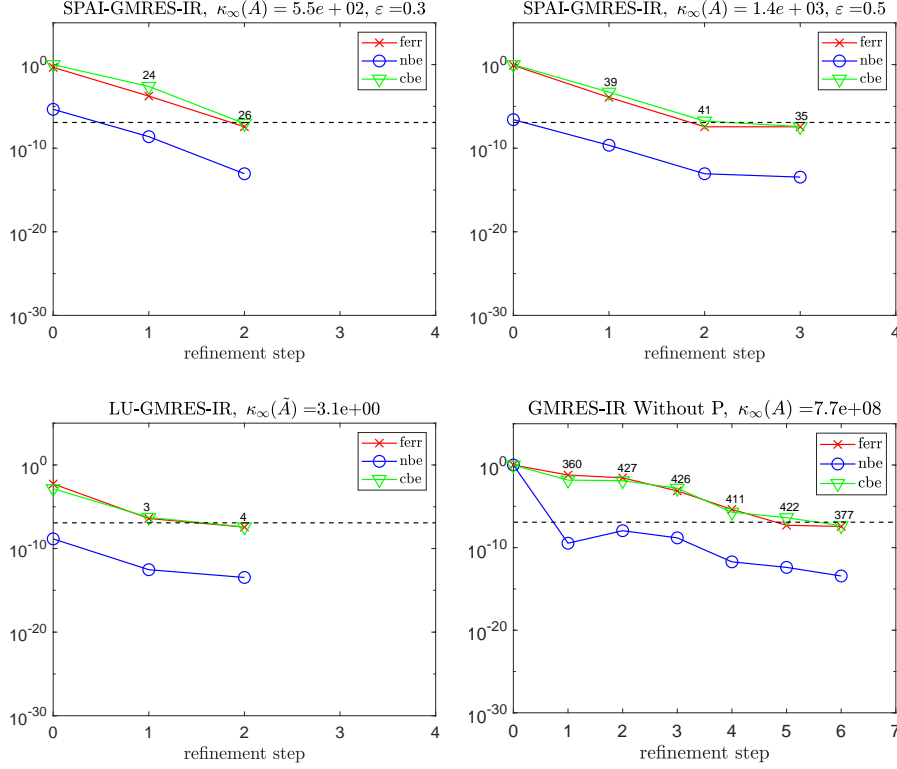


Fig. 4.8: `hor_131` (H, S, D). Convergence of the forward error (ferr), normwise backward error (nbe) and componentwise backward error (cbe) for iterative refinement on a problem with the matrix `hor_131` using SPAI-GMRES-IR with  $\varepsilon = 0.3$  (top left) and  $\varepsilon = 0.5$  (top right), LU-GMRES-IR (bottom left), and GMRES-IR with no preconditioning (bottom right), using precisions  $(u_f, u, u_r) = (\text{half}, \text{single}, \text{double})$ . Numbers on data markers give the number of GMRES iterations in the given refinement step.

Table 4.9: `hor_131` (H, S, D). Comparison of SPAI-GMRES-IR for different  $\varepsilon$  values with GMRES-IR with full LU and with no preconditioner for the matrix `hor_131` using  $(u_f, u, u_r) = (\text{half}, \text{single}, \text{double})$ . For this matrix,  $n = 434$ ,  $nnz(A) = 4182$ , and  $nnz(A^{-1}) = 188356$ .

Preconditioner	Precond. $nnz$	GMRES-IR steps/iterations
SPAI ( $\varepsilon = 0.3$ , $\alpha = 30$ , $\beta = 30$ )	29247	50(24, 26)
SPAI ( $\varepsilon = 0.5$ , $\alpha = 30$ , $\beta = 30$ )	9814	115(39, 41, 35)
Full LU	98917	7(3, 4)
None	0	2423(360, 427, 426, 411, 422, 377)

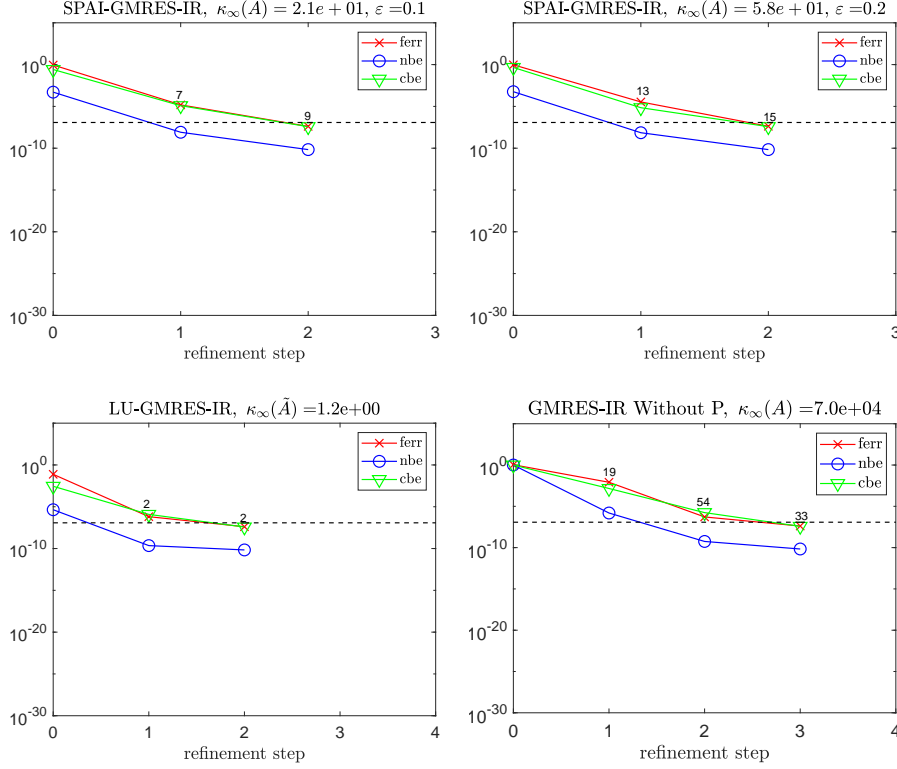


Fig. 4.9: `jpwh_991` (H, S, D). Convergence of the forward error (ferr), normwise backward error (nbe) and componentwise backward error (cbe) for iterative refinement on a problem with the matrix `jpwh_991` using SPAI-GMRES-IR with  $\varepsilon = 0.2$  (top left) and  $\varepsilon = 0.5$  (top right), LU-GMRES-IR (bottom left), and GMRES-IR with no preconditioning (bottom right), using precisions  $(u_f, u, u_r) = (\text{half}, \text{single}, \text{double})$ . Numbers on data markers give the number of GMRES iterations in the given refinement step.

Table 4.10: `jpwh_991` (H, S, D). Comparison of SPAI-GMRES-IR for different  $\varepsilon$  values with GMRES-IR with full LU and with no preconditioner for the matrix `jpwh_991` using  $(u_f, u, u_r) = (\text{half}, \text{single}, \text{double})$ . For this matrix,  $n = 991$ ,  $\text{nnz}(A) = 6027$ , and  $\text{nnz}(A^{-1}) = 833725$ .

Preconditioner	Precond. $\text{nnz}$	GMRES-IR steps/iterations
SPAI ( $\varepsilon = 0.1$ , $\alpha = 50$ , $\beta = 50$ )	75848	16(7, 9)
SPAI ( $\varepsilon = 0.2$ , $\alpha = 50$ , $\beta = 50$ )	16835	28(13, 15)
Full LU	135867	4(2, 2)
None	0	106(19, 54, 33)

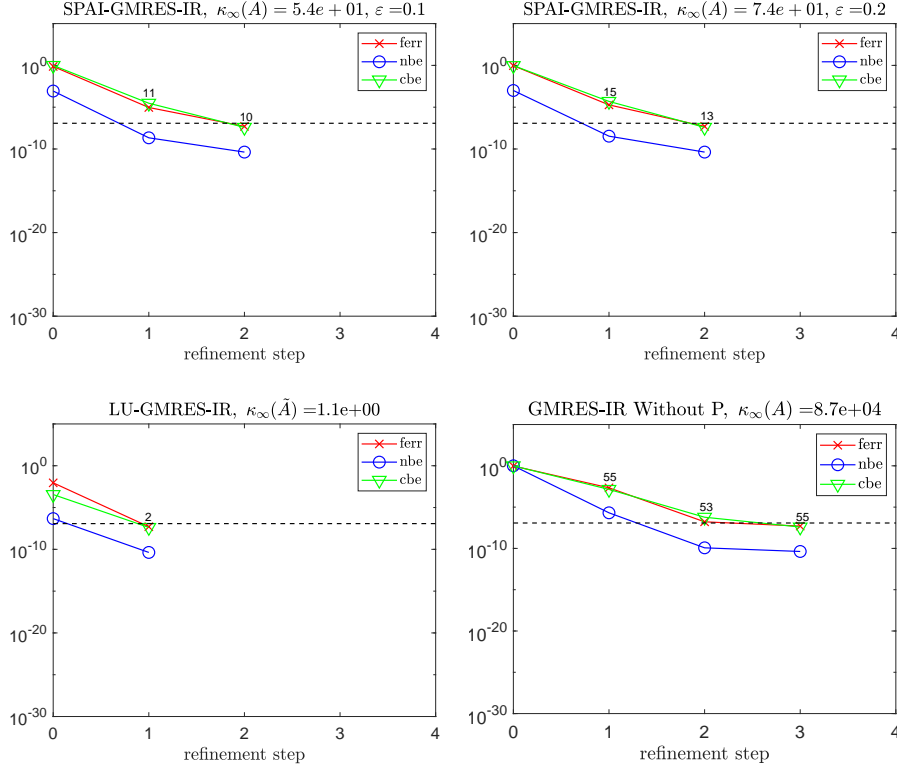


Fig. 4.10: `cdde4` (H, S, D). Convergence of the forward error (ferr), normwise backward error (nbe) and componentwise backward error (cbe) for iterative refinement on a problem with the matrix `cdde4` using SPAI-GMRES-IR with  $\varepsilon = 0.2$  (top left) and  $\varepsilon = 0.5$  (top right), LU-GMRES-IR (bottom left), and GMRES-IR with no preconditioning (bottom right), using precisions  $(u_f, u, u_r) = (\text{half}, \text{single}, \text{double})$ . Numbers on data markers give the number of GMRES iterations in the given refinement step.

Table 4.11: `cdde4` (H, S, D). Comparison of SPAI-GMRES-IR for different  $\varepsilon$  values with GMRES-IR with full LU and with no preconditioner for the matrix `cdde4` using  $(u_f, u, u_r) = (\text{half}, \text{single}, \text{double})$ . For this matrix,  $n = 961$ ,  $\text{nnz}(A) = 4681$ , and  $\text{nnz}(A^{-1}) = 923218$ .

Preconditioner	Precond. $\text{nnz}$	GMRES-IR steps/iterations
SPAI ( $\varepsilon = 0.1$ , $\alpha = 70$ , $\beta = 70$ )	113081	21(11, 10)
SPAI ( $\varepsilon = 0.2$ , $\alpha = 70$ , $\beta = 70$ )	27015	28(15, 13)
SPAI ( $\varepsilon = 0.5$ , $\alpha = 70$ , $\beta = 70$ )	4681	69(37, 32)
Full LU	58681	2(2)
None	0	163(55, 53, 55)

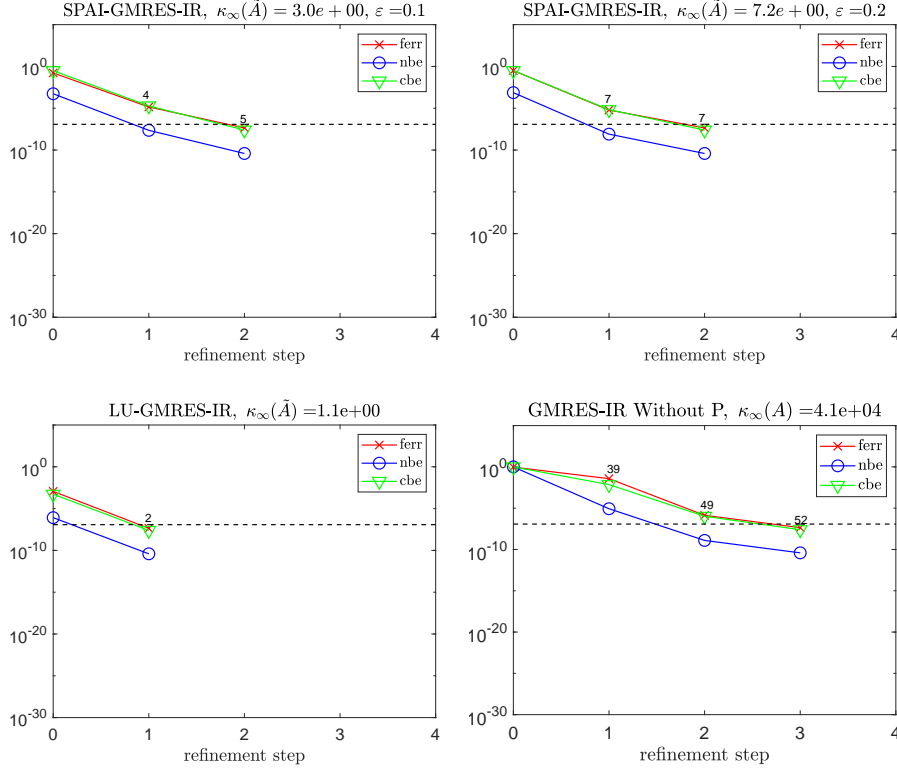


Fig. 4.11: **gre\_115** (H, S, D). Convergence of the forward error (ferr), normwise backward error (nbe) and componentwise backward error (cbe) for iterative refinement on a problem with the matrix **gre\_115** using SPAI-GMRES-IR with  $\varepsilon = 0.2$  (top left) and  $\varepsilon = 0.5$  (top right), LU-GMRES-IR (bottom left), and GMRES-IR with no preconditioning (bottom right), using precisions  $(u_f, u, u_r) = (\text{half}, \text{single}, \text{double})$ . Numbers on data markers give the number of GMRES iterations in the given refinement step.

Table 4.12: **gre\_115** (H, S, D). Comparison of SPAI-GMRES-IR for different  $\varepsilon$  values with GMRES-IR with full LU and with no preconditioner for the matrix **gre\_115** using  $(u_f, u, u_r) = (\text{half}, \text{single}, \text{double})$ . For this matrix,  $n = 115$ ,  $nnz(A) = 421$ , and  $nnz(A^{-1}) = 13225$ .

Preconditioner	Precond. $nnz$	GMRES-IR steps/iterations
SPAI ( $\varepsilon = 0.1$ , $\alpha = 20$ , $\beta = 20$ )	6112	9(4, 5)
SPAI ( $\varepsilon = 0.2$ , $\alpha = 16$ , $\beta = 10$ )	3399	14(7, 7)
SPAI ( $\varepsilon = 0.5$ , $\alpha = 16$ , $\beta = 10$ )	882	59(29, 30)
Full LU	3423	2(2)
None	0	140(39, 49, 52)



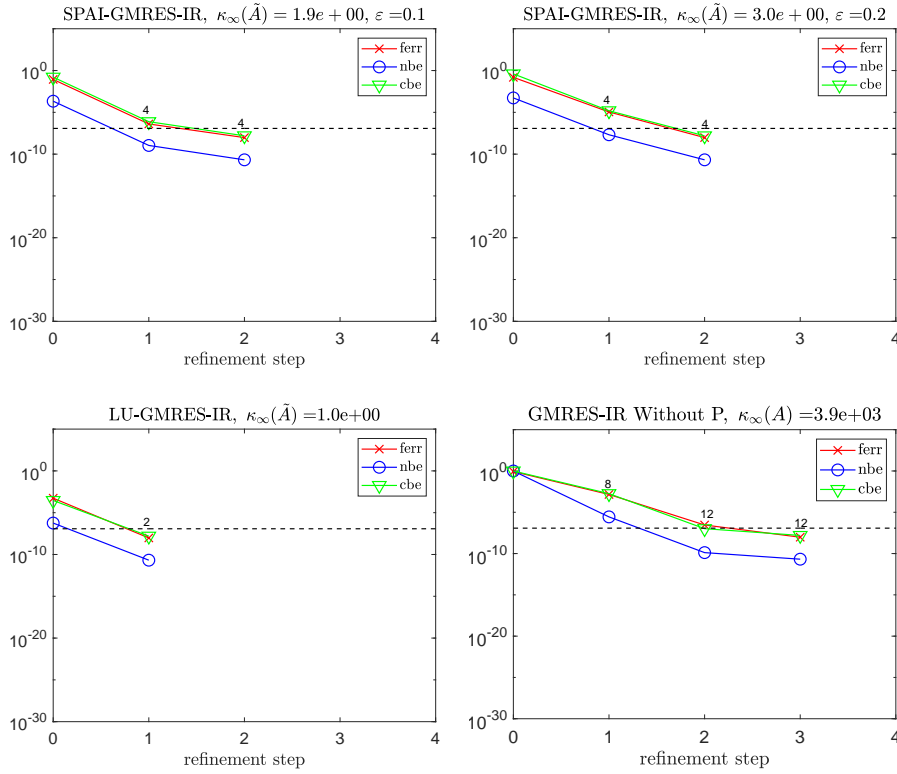


Fig. 4.12: **caget5** (H, S, D). Convergence of the forward error (ferr), normwise backward error (nbe) and componentwise backward error (cbe) for iterative refinement on a problem with the matrix **caget5** using SPAl-GMRES-IR with  $\varepsilon = 0.1$  (top left) and  $\varepsilon = 0.2$  (top right), LU-GMRES-IR (bottom left), and GMRES-IR with no preconditioning (bottom right), using precisions  $(u_f, u, u_r) = (\text{half}, \text{single}, \text{double})$ . Numbers on data markers give the number of GMRES iterations in the given refinement step.

Table 4.13: **caget5** (H, S, D). Comparison of SPAl-GMRES-IR for different  $\varepsilon$  values with GMRES-IR with full LU and with no preconditioner for the matrix **caget5** using  $(u_f, u, u_r) = (\text{half}, \text{single}, \text{double})$ . For this matrix,  $n = 37$ ,  $\text{nnz}(A) = 421$ , and  $\text{nnz}(A^{-1}) = 1369$ .

Preconditioner	Precond. $\text{nnz}$	GMRES-IR steps/iterations
SPAl ( $\varepsilon = 0.1, \alpha = 20, \beta = 20$ )	421	8(4, 4)
SPAl ( $\varepsilon = 0.2, \alpha = 20, \beta = 20$ )	255	8(4, 4)
Full LU	489	2(2)
None	0	32(8, 12, 12)

**4.3. Experiments with  $(u_f, u, u_r) = (\text{single}, \text{single}, \text{double})$ .** We now test three of the same problems used in Section 4.2, now using single precision instead of half precision for  $u_f$ . The analysis in Section 3 indicates that as long as, say, half precision is sufficient for producing a preconditioner satisfying (3.4), there is in general no expected benefit to using higher precision in the SPAI construction in terms of preconditioner quality. We do recall, however, that the number of nonzeros in the preconditioner may be different when higher versus lower precision is used. For easy comparison, in the tables for these experiments, we give in red bracketed format the equivalent values from Tables in Section 4.2.

We show results for the matrix **bfwa782** in Figure 4.13 and Table 4.14. Comparing these results with Table 4.8 for the SPAI preconditioners, the number of nonzeros changes slightly, but not significantly for  $u_f$  single versus  $u_f$  half. Further, the number of total GMRES iterations is nearly unchanged (requiring 3 more iterations when  $\varepsilon = 0.5$  and 3 fewer iterations when  $\varepsilon = 0.2$  for single versus half precision). This is in contrast to the case of LU preconditioning, where the precision used for the LU factorization makes a significant difference in preconditioner quality; using  $u_f = \text{half}$  requires  $7\times$  more iterations than  $u_f = \text{single}$  for LU-GMRES-IR. This intuitively makes sense since LU factorization is a direct algorithm rather than an iterative one like SPAI that iterates until the stopping criterion is met.

For the matrix **hor\_131** (Figure 4.14, Table 4.15), comparing with Table 4.9, we do observe more significant differences in the size of the SPAI preconditioners computed in half versus single precision. The SPAI preconditioners computed in half precision have about  $1.15\times$  more nonzeros than those computed in single precision. SPAI-GMRES-IR also performs slightly better with the preconditioners computed in single precision, despite having fewer nonzero entries. SPAI-GMRES-IR with  $u_f = \text{half}$  requires  $1.04\times$  more GMRES iterations for  $\varepsilon = 0.3$  and  $1.42\times$  more iterations for  $\varepsilon = 0.5$  versus SPAI-GMRES-IR with  $u_f = \text{single}$ . These differences are not particularly significant. Again, there is a greater difference in the LU-GMRES-IR case, where using  $u_f = \text{half}$  results in  $7\times$  more GMRES iterations than  $u_f = \text{single}$ .

Finally, for **cdde4** (Figure 4.15, Table 4.16), comparing with Table 4.11, we in general see very little difference between  $u_f$  single and  $u_f$  half. Notice that while for SPAI-GMRES-IR with  $\varepsilon = 0.1$ , with  $u_f = \text{half}$ ,  $M$  has more nonzeros, and more GMRES iterations are required than with  $u_f = \text{single}$ . However, for SPAI-GMRES-IR with  $\varepsilon = 0.2$ ,  $u_f = \text{half}$  requires in an  $M$  with more nonzeros but slightly fewer GMRES iterations than  $u_f = \text{single}$ . This indicates that there is no hard-and-fast rule that higher precision is necessarily better. Perhaps most perplexing is that case where  $\varepsilon = 0.5$ . Here, the  $M$  matrices produced using both  $u_f = \text{half}$  and  $u_f = \text{single}$  have the same number of nonzeros, but for some reason the case with  $u_f = \text{half}$  results in 13 fewer GMRES iterations. We are unsure as to why this behavior occurs. Note that here, the behavior of LU-GMRES-IR is also nearly the same for both cases, requiring 2 GMRES iterations for  $u_f = \text{half}$  versus 1 for  $u_f = \text{single}$ , presumably because the matrix is very well conditioned.

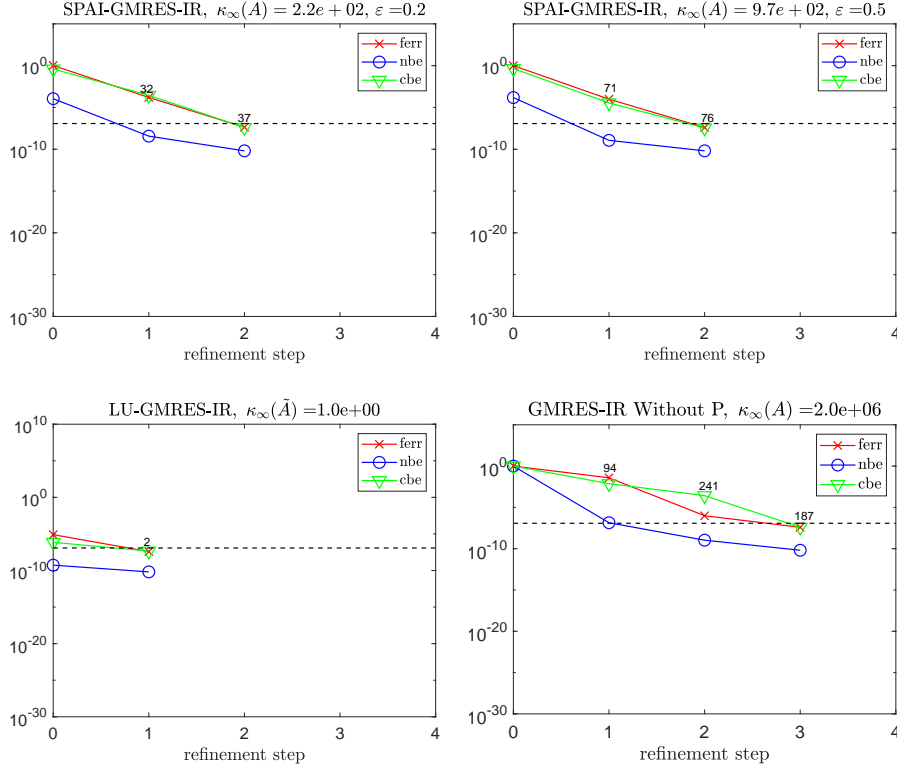


Fig. 4.13: **bfw782** (S, S, D). Convergence of the forward error (ferr), normwise backward error (nbe) and componentwise backward error (cbe) for iterative refinement on a problem with the matrix **bfw782** using SPAI-GMRES-IR with  $\varepsilon = 0.2$  (top left) and  $\varepsilon = 0.5$  (top right), LU-GMRES-IR (bottom left), and GMRES-IR with no preconditioning (bottom right), using precisions  $(u_f, u, u_r) = (\text{single}, \text{single}, \text{double})$ . Numbers on data markers give the number of GMRES iterations in the given refinement step.

Table 4.14: **bfw782** (S, S, D). Comparison of SPAI-GMRES-IR for different  $\varepsilon$  values with GMRES-IR with full LU and with no preconditioner for the matrix **bfw782** using  $(u_f, u, u_r) = (\text{single}, \text{single}, \text{double})$ . For this matrix,  $n = 782$ ,  $\text{nnz}(A) = 7514$ , and  $\text{nnz}(A^{-1}) = 458839$ . Bracketed red numbers give the equivalent values for the case  $u_f = \text{half}$ ; see Table 4.8.

Preconditioner	Precond. $\text{nnz}$	GMRES-IR steps/iterations
SPAI ( $\varepsilon = 0.2$ , $\alpha = 70$ , $\beta = 70$ )	26782 [28077]	69(32, 37) [66]
SPAI ( $\varepsilon = 0.5$ , $\alpha = 70$ , $\beta = 70$ )	7529 [7528]	147(71, 76) [151]
Full LU	347828	1(1) [7]
None	0	522(94, 241, 187)

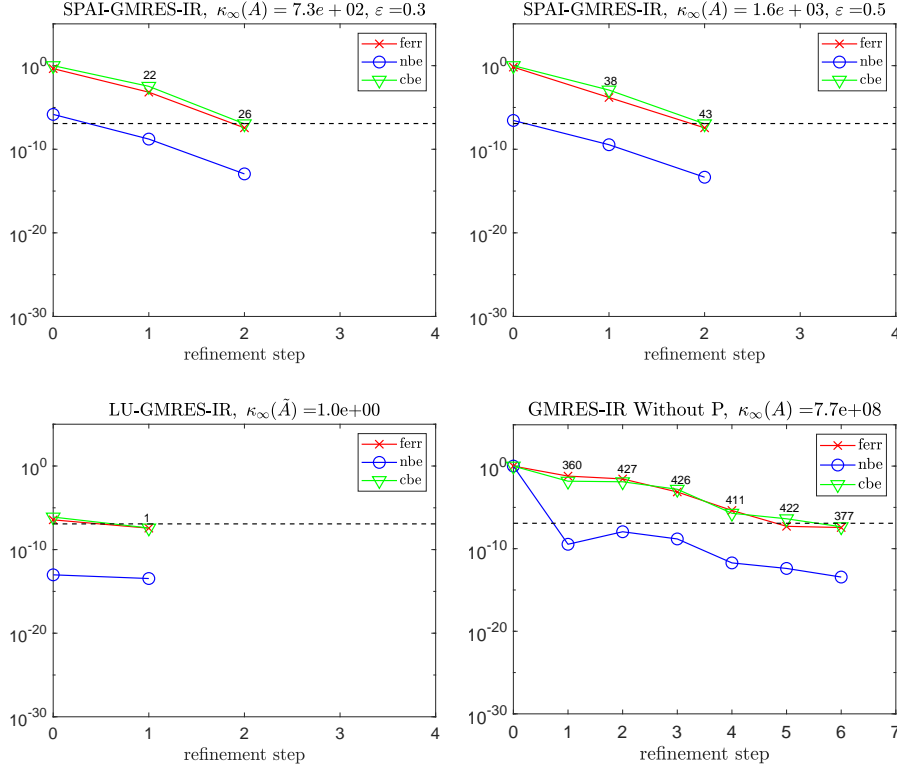


Fig. 4.14: `hor_131` (S, S, D). Convergence of the forward error (ferr), normwise backward error (nbe) and componentwise backward error (cbe) for iterative refinement on a problem with the matrix `hor_131` using SPAI-GMRES-IR with  $\varepsilon = 0.1$  (top left) and  $\varepsilon = 0.3$  (top right), LU-GMRES-IR (bottom left), and GMRES-IR with no preconditioning (bottom right), using precisions  $(u_f, u, u_r) = (\text{single}, \text{single}, \text{double})$ . Numbers on data markers give the number of GMRES iterations in the given refinement step.

Table 4.15: `hor_131` (S, S, D). Comparison of SPAI-GMRES-IR for different  $\varepsilon$  values with GMRES-IR with full LU and with no preconditioner for the matrix `hor_131` using  $(u_f, u, u_r) = (\text{single}, \text{single}, \text{double})$ . For this matrix,  $n = 434$ ,  $\text{nnz}(A) = 4182$ , and  $\text{nnz}(A^{-1}) = 188,356$ . Bracketed red numbers give the equivalent values for the case  $u_f = \text{half}$ ; see Table 4.9.

Preconditioner	Precond. $\text{nnz}$	GMRES-IR steps/iterations
SPAI ( $\varepsilon = 0.3$ , $\alpha = 30$ , $\beta = 30$ )	25977 [29247]	48(22, 26) [50]
SPAI ( $\varepsilon = 0.5$ , $\alpha = 30$ , $\beta = 30$ )	8541 [9814]	81(38, 43) [115]
Full LU	98917	1(1) [7]
None	0	2423(360, 427, 426, 411, 422, 377)

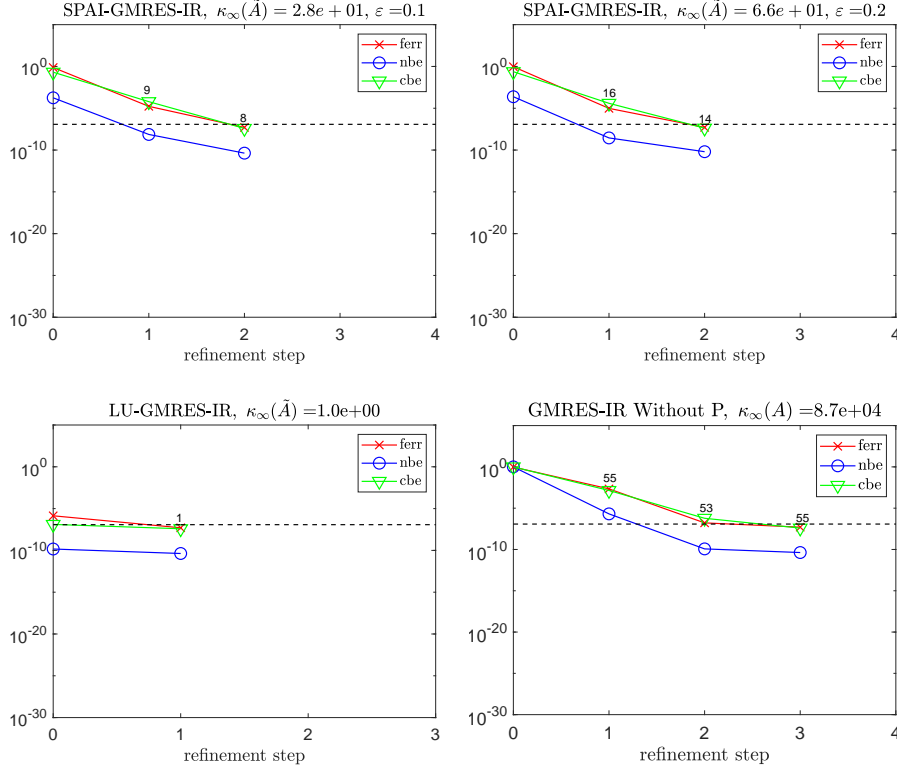


Fig. 4.15: `cdd4` (S, S, D). Convergence of the forward error (ferr), normwise backward error (nbe) and componentwise backward error (cbe) for iterative refinement on a problem with the matrix `cdd4` using SPAI-GMRES-IR with  $\varepsilon = 0.2$  (top left) and  $\varepsilon = 0.5$  (top right), LU-GMRES-IR (bottom left), and GMRES-IR with no preconditioning (bottom right), using precisions  $(u_f, u, u_r) = (\text{single}, \text{single}, \text{double})$ . Numbers on data markers give the number of GMRES iterations in the given refinement step.

Table 4.16: `cdd4` (S, S, D). Comparison of SPAI-GMRES-IR for different  $\varepsilon$  values with GMRES-IR with full LU and with no preconditioner for the matrix `cdd4` using  $(u_f, u, u_r) = (\text{single}, \text{single}, \text{double})$ . For this matrix,  $n = 961$ ,  $\text{nnz}(A) = 4681$ , and  $\text{nnz}(A^{-1}) = 923218$ . Bracketed red numbers give the equivalent values for the case  $u_f = \text{half}$ ; see Table 4.11.

Preconditioner	Precond. $\text{nnz}$	GMRES-IR steps/iterations
SPAI ( $\varepsilon = 0.1$ , $\alpha = 70$ , $\beta = 70$ )	105635 [113081]	17(9, 8) [21]
SPAI ( $\varepsilon = 0.2$ , $\alpha = 70$ , $\beta = 70$ )	26880 [27015]	30(16, 14) [28]
SPAI ( $\varepsilon = 0.5$ , $\alpha = 70$ , $\beta = 70$ )	4681 [4681]	82(43, 39) [69]
Full LU	58681	1(1) [2]
None	0	163(55, 53, 55)

**5. Conclusions and future work.** In this work we explored the use of sparse approximate inverse preconditioners within mixed precision GMRES-based iterative refinement as a method of solving sparse linear systems. Our numerical experiments suggest that SPAI preconditioning may in some cases offer a performance advantage versus using a full LU factorization; although the number of refinement steps needed for convergence may increase, the preconditioner used in each iteration of GMRES may be considerably sparser and thus less expensive to apply.

We have analyzed the computation of an SPAI preconditioner in some finite precision  $u_f$ . The stopping criterion used in constructing each column of the sparse approximate inverse  $M$  is based on the size of the measured residual norm  $e_k - Am_k$  being less than some user-specified parameter  $\varepsilon$ . Thus for a given  $\varepsilon$ , our analysis shows that we must use  $u_f \lesssim \varepsilon \text{cond}_2^{-1}(A^T)$  in order to guarantee that this stopping criterion can be achieved. As long as this constraint on  $u_f$  holds, then the computed  $\widehat{M}$  satisfies the bounds proved for the exact arithmetic case in [20] up to a constant factor. An interesting point is that there is no significant benefit in terms of resulting preconditioner quality to using a precision higher than dictated by this level.

We briefly give bounds for the case that the stopping criteria used is based on a maximum specified sparsity structure rather than the residual norm in each column. In this case, the bounds rely on knowledge of the corresponding achievable  $\varepsilon$  for the given sparsity structure assuming exact arithmetic.

We then prove conditions under which GMRES left preconditioned by the SPAI preconditioner, which we call SPAI-GMRES-IR, will be backward stable with respect to the preconditioned system. As long as the constraint  $u_f \lesssim \varepsilon \text{cond}_2(A^T)$  is satisfied, meaning that an approximate preconditioner with parameter  $\varepsilon$  is computable in precision  $u_f$ , then the constraints for convergence of SPAI-GMRES-IR are essentially the same as those for GMRES-IR given in [11].

Although we have considered the case here where, within GMRES, the preconditioner and preconditioned linear system is applied to a vector in double the working precision (the same assumption used in [10, 11], this may not be necessary in practice. Bounds for a more general five-precision GMRES-IR algorithm, for which uniform-precision GMRES is a special case, were derived in [3]. This case could easily be handled for the SPAI-GMRES-IR algorithm as well.

In [25], the authors develop sophisticated scaling strategies for prescaling a matrix before converting to half precision, where parameters are chosen to account for pivot growth in the low-precision LU factorization within GMRES-IR. We have not considered any scaling here, and restrict our test problems to those which do not exhibit over/underflow when converting to lower precision. However, we believe that there is opportunity for developing and incorporating scaling strategies based on the computations within the SPAI construction as well.

Finally, it is clear that other approximate preconditioners, such as incomplete LU factorization, factorized sparse approximate inverses, or sparse approximate inverses based on a fixed sparsity pattern may be suitable use within mixed precision Krylov-subspace-based iterative refinement schemes. We have started with one variant of sparse approximate inverses here, but plan to study other approximate preconditioners in the future.

## REFERENCES

- [1] A. ABDELFAH, H. ANZT, E. G. BOMAN, E. CARSON, T. COJEAN, J. DONGARRA, A. FOX, M. GATES, N. J. HIGHAM, X. S. LI, ET AL., *A survey of numerical linear algebra methods utilizing mixed-precision arithmetic*, Int. J. High Perf. Comput. Appl., 35 (2021), pp. 344–369.
- [2] A. ABDELFAH, H. ANZT, J. DONGARRA, M. GATES, A. HAIDAR, J. KURZAK, P. LUSZCZEK, S. TOMOV, I. YAMAZAKI, AND A. YARKHAN, *Linear algebra software for large-scale accelerated multicore computing*, Acta Numerica, 25 (2016), pp. 1–160.
- [3] P. AMESTOY, A. BUTTARI, N. J. HIGHAM, J.-Y. L’EXCELLENT, T. MARY, AND B. VIEUBLÉ, *Five-precision GMRES-based iterative refinement*, MIMS EPrint 2021.5, Manchester Institute for Mathematical Sciences, The University of Manchester, Manchester, UK, apr 2021.
- [4] P. AMESTOY, A. BUTTARI, N. J. HIGHAM, J.-Y. L’EXCELLENT, T. MARY, AND B. VIEUBLÉ, *Combining sparse approximate factorizations with mixed precision iterative refinement*, working paper or preprint, Jan. 2022, <https://hal.archives-ouvertes.fr/hal-03536031>.
- [5] H. ANZT, T. K. HUCKLE, J. BRÄCKLE, AND J. DONGARRA, *Incomplete sparse approximate inverses for parallel preconditioning*, Par. Comput., 71 (2018), pp. 1–22.
- [6] S. T. BARNARD, L. M. BERNARDO, AND H. D. SIMON, *An MPI implementation of the SPAI preconditioner on the T3E*, Int. J. High Perf. Comput. Appl., 13 (1999), pp. 107–123.
- [7] M. BENZI, *Preconditioning techniques for large linear systems: a survey*, J. Comput. Phys., 182 (2002), pp. 418–477.
- [8] M. BENZI AND M. TŪMA, *A sparse approximate inverse preconditioner for nonsymmetric linear systems*, SIAM J. Sci. Comput., 19 (1998), pp. 968–994.
- [9] M. BENZI AND M. TŪMA, *A comparative study of sparse approximate inverse preconditioners*, Appl. Numer. Math., 30 (1999), pp. 305–340.
- [10] E. CARSON AND N. J. HIGHAM, *A new analysis of iterative refinement and its application to accurate solution of ill-conditioned sparse linear systems*, SIAM J. Sci. Comput., 39 (2017), pp. A2834–A2856.
- [11] E. CARSON AND N. J. HIGHAM, *Accelerating the solution of linear systems by iterative refinement in three precisions*, SIAM J. Sci. Comput., 40 (2018), pp. A817–A847.
- [12] E. CHOW, *Parallel implementation and performance characteristics of sparse approximate inverse preconditioners with a priori sparsity patterns*, Int. J. High Perform. Comput. Appl., 15 (2001), pp. 10–1177.
- [13] J. COSGROVE, J. DÍAZ, AND A. GRIEWANK, *Approximate inverse preconditionings for sparse linear systems*, Int. J. Comput. Math., 44 (1992), pp. 91–110.
- [14] T. A. DAVIS AND Y. HU, *The university of Florida sparse matrix collection*, ACM Trans. Math. Soft., 38 (2011), pp. 1–25.
- [15] M. M. DEHNAVI, D. M. FERNANDEZ, J.-L. GAUDIOT, AND D. D. GIANNACOPOULOS, *Parallel sparse approximate inverse preconditioning on graphic processing units*, IEEE Trans. Par. Dist. Sys., 24 (2012), pp. 1852–1862.
- [16] J. GAO, Q. CHEN, AND G. HE, *A thread-adaptive sparse approximate inverse preconditioning algorithm on multi-GPUs*, Par. Comput., 101 (2021), p. 102724.
- [17] J. GAO, K. WU, Y. WANG, P. QI, AND G. HE, *GPU-accelerated preconditioned GMRES method for two-dimensional Maxwell’s equations*, Int. J. Comput. Math., 94 (2017), pp. 2122–2144.
- [18] N. I. GOULD AND J. A. SCOTT, *Sparse approximate-inverse preconditioners using norm-minimization techniques*, SIAM J. Sci. Comput., 19 (1998), pp. 605–625.
- [19] A. GREENBAUM, V. PTÁK, AND Z. STRAKOŠ, *Any nonincreasing convergence curve is possible for gmres*, SIAM J. Matrix Anal. Appl., 17 (1996), pp. 465–469.
- [20] M. J. GROTE AND T. HUCKLE, *Parallel preconditioning with sparse approximate inverses*, SIAM J. Sci. Comput., 18 (1997), pp. 838–853.
- [21] G. HE, R. YIN, AND J. GAO, *An efficient sparse approximate inverse preconditioning algorithm on GPU*, Concurrency and Computation: Practice and Experience, 32 (2020), p. e5598.
- [22] N. J. HIGHAM, *Accuracy and Stability of Numerical Algorithms*, Society for Industrial and Applied Mathematics, Philadelphia, PA, USA, second ed., 2002.
- [23] N. J. HIGHAM AND T. MARY, *A new preconditioner that exploits low-rank approximations to factorization error*, SIAM J. Sci. Comput., 41 (2019), pp. A59–A82.
- [24] N. J. HIGHAM AND T. MARY, *Solving block low-rank linear systems by LU factorization is numerically stable*, IMA J. Numer. Anal., (2020), pp. 1–30.
- [25] N. J. HIGHAM, S. PRANESH, AND M. ZOUNON, *Squeezing a matrix into half precision, with an*



- application to solving linear systems*, SIAM J. Sci. Comput., 41 (2019), pp. A2536–A2551.
- [26] T. HUCKLE, *Factorized sparse approximate inverses for preconditioning*, J. Supercomput., 25 (2003), pp. 109–117.
  - [27] T. HUCKLE AND A. KALLISCHKO, *Frobenius norm minimization and probing for preconditioning*, Int. J. Comput. Math., 84 (2007), pp. 1225–1248.
  - [28] M. JANKOWSKI AND H. WOŹNIAKOWSKI, *Iterative refinement implies numerical stability*, BIT Numer. Math., 17 (1977), pp. 303–311.
  - [29] J. LANGOU, J. LANGOU, P. LUSZCZEK, J. KURZAK, A. BUTTARI, AND J. DONGARRA, *Exploiting the performance of 32 bit floating point arithmetic in obtaining 64 bit accuracy (revisiting iterative refinement for linear systems)*, in Proc. 2006 ACM/IEEE Conf. Supercomput., 2006.
  - [30] N. LINDQUIST, P. LUSZCZEK, AND J. DONGARRA, *Accelerating restarted GMRES with mixed precision arithmetic*, IEEE Trans. Par. Dist. Sys., 33 (2022), pp. 1027–1037.
  - [31] M. LUKASH, K. RUPP, AND S. SELBERHERR, *Sparse approximate inverse preconditioners for iterative solvers on GPUs*, in Proc. 2012 Symp. High Perf. Comput., Society for Computer Simulation San Diego, CA, USA, 2012, p. 13.
  - [32] C. B. MOLER, *Iterative refinement in floating point*, J. ACM, 14 (1967), pp. 316–321.
  - [33] *Multiprecision Computing Toolbox*. Advanpix, Tokyo. <http://www.advanpix.com>.
  - [34] M. SEDLACEK, *Sparse approximate inverses for preconditioning, smoothing, and regularization*, PhD thesis, Technische Universität München, 2012.
  - [35] R. D. SKEEL, *Iterative refinement implies numerical stability for Gaussian elimination*, Math. Comput., 35 (1980), pp. 817–832.
  - [36] J. H. WILKINSON, *Progress report on the Automatic Computing Engine*, Report MA/17/1024, Mathematics Division, Department of Scientific and Industrial Research, National Physical Laboratory, Teddington, UK, Apr. 1948.
  - [37] J. H. WILKINSON, *Rounding Errors in Algebraic Processes*, Notes on Applied Science No. 32, Her Majesty's Stationery Office, London, 1963. Also published by Prentice-Hall, Englewood Cliffs, NJ, USA. Reprinted by Dover, New York, 1994.